Journal of Futures Markets

WILEY

RESEARCH ARTICLE

A Generalized Error Distribution-Copula Framework for Pricing Chinese Treasury Bond Futures With Embedded Options

Xiaofeng Yang

School of Economics, Hangzhou Normal University, Hangzhou, China

Correspondence: Xiaofeng Yang (xiaofengyang@hznu.edu.cn)

Received: 20 November 2024 | **Revised:** 31 October 2025 | **Accepted:** 10 November 2025

Keywords: generalized error distribution | institutional coordination | Monte Carlo simulation | Student's *t*-Copula | treasury bond futures

ABSTRACT

This study investigates the pricing of complex embedded options—quality, rolling timing, and month-end timing options—in China's Treasury bond futures market. We develop an innovative pricing model that integrates the generalized error distribution (GED) and Copula functions, specifically designed to capture the unique dependencies arising from institutional coordination. The framework models "valuation deviations"—discrepancies between actual closing prices and ChinaBond valuations—using GED marginals, while the Student's *t*-Copula explicitly captures symmetric heavy-tailed dependence patterns induced by coordinated institutional behavior. Empirical analysis demonstrates that the model achieves superior pricing accuracy compared to traditional approaches by effectively capturing policy-shaped joint distribution characteristics. Furthermore, we introduce a policy adjustment term to account for systematic mispricing during periods of strong policy guidance, further enhancing the model's robustness. This research provides a reliable valuation benchmark tailored to constrained market structures and advances pricing theory for derivatives markets influenced by institutional and policy factors.

JEL Classification: G12, G13, C58, C63, G17

1 | Introduction

The Treasury bond futures market stands as a cornerstone in the intricate landscape of modern finance, offering investors a powerful derivative instrument for managing interest rate risks. With the market's relentless progression towards maturity and stability, the financial sector has increasingly turned its focus to refining the art of predicting Treasury bond futures prices. Pricing models are continuously refined to adapt to evolving market dynamics. However, these models must account for distinct institutional frameworks. China's market operates under unique constraints:

State-Dominated Participation: Financial institutions owned or controlled by the state (e.g., major commercial banks, policy banks) dominate trading, holding over 63% of open interest (CFFEX Yearbook 2024). Their actions are often influenced by policy directives, leading to coordinated behavior.

Capital Controls & Limited Foreign Access: Strict Qualified Foreign Institutional Investor (QFII) quotas significantly restrict foreign participation, contrasting sharply with liberalized markets like the US.

Regulatory Design & Policy Intervention: Key design features include: (1) The Short Position Delivery Selection System granting exclusive timing and quality options to sellers; (2) Synchronized trading/delivery deadlines (e.g., 15:15 cutoff), eliminating the "Wild Card Play" option[1] prevalent in other markets; 3) Active window guidance by regulators (the People's Bank of China (PBOC) and the China Securities Regulatory Commission (CSRC)) and liquidity operations (e.g., Ministry of

Finance bond selling) to stabilize markets. This institutional structure fundamentally shapes price dynamics.

These institutional features induce specific statistical characteristics crucial for pricing:

Synchronized Behavior & Heavy Tails: Policy coordination among dominant state institutions (> 63% open interest) generates heavy-tailed co-movement in "valuation deviations"—distinct from random tail risks in decentralized markets. Critically, this dependence emerges from policy-coordinated institutional behavior (e.g., entities responding to unified directives), not stochastic market discovery. Traditional models assuming i.i.d. normal distributions or decentralized price discovery fail to capture this mechanistic structure. Our model explicitly parameterizes these policy-induced statistical regularities, as evidenced by extreme kurtosis observations (e.g., 137.79 for Bond 9 in T2503).

Treasury bond futures, a distinctive interest rate option, stand apart in that while the underlying is a standardized nominal bond, the actual delivery includes a range of Treasury bonds that meet specific market criteria. This delivery mechanism grants the short position the right to select both the delivery date and the specific bonds, thereby endowing Treasury bond futures with three crucial embedded options: the quality option, the rolling timing option, and the month-end timing option. These embedded options significantly complicate the pricing process of Treasury bond futures compared to traditional futures contracts. Pricing such futures requires not only an assessment of the underlying asset's price fluctuations but also a thorough consideration of how these embedded options impact the overall value, thereby increasing the complexity and challenge for pricing models. In China's institutional context, where sellers hold exclusive control and policy coordination is high, accurately modeling the joint distribution of deliverable bond valuation deviations becomes paramount.

In their groundbreaking working paper, Yang and Zhao (2025) tackle this pricing challenge head-on. They begin by analyzing the "valuation deviations" of each deliverable bond, proposing that these deviations follow an independent and identically distributed (i.i.d.) generalized error distribution. By integrating these three embedded options into a cohesive framework, they introduce a novel pricing model grounded in the GED distribution and integrated options. This approach outperforms traditional normal distribution assumptions by better capturing the distribution characteristics of "valuation deviations" in deliverable bonds, thereby improving pricing accuracy.

However, their i.i.d. assumption overlooks the significant, policy-induced dependence observed in China's market where synchronized institutional behavior creates strong correlations in valuation deviations across deliverable bonds. To address this limitation, we incorporate a Copula function to capture the intricate interdependence. The symmetric heavy-tailed nature of this dependence, evidenced by high joint kurtosis, specifically motivates our selection of the Student's *t*-Copula. Furthermore, we introduce a policy adjustment term to correct for the systematic pricing bias induced by policy interventions—a mechanism that can rationally sustain market mispricing.

This research endeavor aims to develop a pricing model that better reflects market realities, explicitly tailored to the institutional realities of China's policy-influenced Treasury futures market. By harmoniously blending the GED distribution assumption with the Copula functions and leveraging Monte Carlo simulation techniques, we aim to simulate future "valuation deviations" scenarios and embed them within our integrated option pricing model. Leveraging Monte Carlo simulation, and explicitly embedding a policy adjustment mechanism, this methodology promises to deliver more precise Treasury bond futures price estimates for markets characterized by coordinated institutional behavior and policy intervention.

The article unfolds in a systematic manner, first exploring the research's backdrop, challenges, and significance. It then delves into a comprehensive review of relevant literature and theoretical foundations. Subsequently, the model's construction process is detailed, encompassing the GED distribution premise and the application of the Copula functions. Following this, simulation experiments and empirical analyses are conducted to evaluate the model's efficacy, highlighting its strengths and areas for improvement. Finally, the study summarizes its key findings, highlights research contributions, and suggests directions for future research.

2 | Literature Review

2.1 | Development of Treasury Bond Futures Pricing Models

The cost of carry model, introduced by Cornell and French (1983), provides a foundational framework for pricing stock index futures, defining futures prices as the difference between spot prices and holding costs, adjusted for cash interest and dividend income. Kawaller and Koch (1984) extended this model to Treasury bond futures, demonstrating its predictive accuracy. However, the model's limitation lies in its neglect of embedded options, which significantly impact pricing precision.

Subsequent research has focused on the four embedded options in Treasury futures pricing, particularly quality options. Margrabe (1978) laid the theoretical groundwork with the exchange option pricing model, later applied to Treasury bond futures by Hemler (1990). Grieves and Marcus (2005) validated the model's efficacy under a flat yield curve, while Carr (1988) and Carr and Chen (1996) enhanced precision using factor models. Ritchken and Sankarasubramanian (1992) further advanced the field with the HJM model (Heath et al. (1992)). Contributions from Kane and Marcus (1986a), Nunes and Oliveira (2007), and Rendleman (2004) have collectively enriched the theoretical framework for pricing quality options.

Timing options, including rolling timing, month-end timing, and Wild Card Play options, are equally complex. Scholars have employed numerical methods, such as lattice models, to address their pricing intricacies. Boyle (1989) introduced a pioneering two-stage model for rolling timing options, while Biagini and Björk (2007) developed an innovative framework for pricing in incomplete markets. Broadie and Sundaresan (1987) utilized lattice models to rigorously analyze month-end timing options, and Cohen (1995) and Kane and Marcus (1986b) conducted foundational studies on Wild Card Play options. Additionally, research by Chen and Yeh (2012), Gay and Manaster (1986), Lindensjö (2016), and Ben-Abdallah et al. (2012) has explored the combined impact of multiple options on Treasury bond

futures pricing, offering a nuanced understanding of these mechanisms.

2.2 | Application of Generalized Error Distribution (GED)

The GED has gained prominence for its ability to model financial time series with fat-tailed and non-normal characteristics. Jiang and Hua (2019) integrated GED with the TGARCH-M model to refine option pricing, capturing multi-frequency risks and information asymmetry. Fan et al. (2008) applied the GED-GARCH model to assess crude oil market risks, while Ampadu et al. (2024) highlighted its advantages in financial time series modeling.

Liao et al. (2014) extended GED to extreme value statistics, and Marček et al. (2019) incorporated it into RBF neural networks for improved financial predictions. Zhang (2013) applied GED to Bayesian growth curve models in biostatistics and medicine. The asymmetric GED (AGED), proposed by Abebe and Goshu (2024), further enhances its flexibility. Theoretical contributions by Zou et al. (2023) and Lu et al. (2024) have advanced understanding of GED's asymptotic behavior, while Coin (2017) developed a GED goodness-of-fit test.

2.3 | Application of Copula Functions in Financial Market

Copula models have become essential for analyzing asset dependence and risk management. Zhang et al. (2022) used the DCC-GARCH *t*-Copula model to study dependencies between ESG stock indices, energy stock indices, and carbon emission futures. Kouaissah et al. (2022) and Kim et al. (2020) expanded Copula applications to portfolio selection and debt market analysis. Fernandes et al. (2021) applied a stochastic-copula framework to model the dependence between electricity and natural gas prices during the energy transition, identifying Clayton and Student's t-copulas as the most suitable for energy risk management.

Liu et al. (2019) explored cross-market dependence between U.S. stocks and Treasury bonds, while Metin Karakas (2019, 2022) analyzed commodity-stock market interdependencies using Copula-GARCH and Vine Copula methods. Yu et al. (2025) introduced a fuzzy Copula-GMM model for salmon futures hedging, and Muganda et al. (2023) integrated dynamic conditional Copulas into option pricing. Chang and Zhang (2018) examined asymmetric tail dependence in China's carbon emission allowances using a GARCH Copula model with GED.

2.4 | Literature Commentary

Existing literature has extensively explored Treasury bond futures pricing, including the cost of carry model and embedded options. However, traditional models often fail to capture nonlinear dependencies and non-normal behavior, particularly in extreme market conditions. The GED and Copula models offer promising solutions: GED excels in modeling fat-tailed financial data, while Copulas effectively capture multivariate dependencies.

This study integrates GED and Copula models to price Treasury bond futures, leveraging the GED's ability to model non-normal characteristics and Copulas' capacity to construct dependence structures among deliverable bonds. This approach aims to provide a more accurate representation of Treasury bond futures price dynamics, offering improved tools for investors and risk management institutions.

3 | Copula and GED-Based Framework for Pricing Treasury Bond Futures

3.1 | Treasury Bond Future and Its Embedded Options

Treasury bond futures, as essential interest rate derivatives with the Treasury bonds as their underlying assets, play a pivotal role in the financial market. Their evolutionary journey has mirrored the remarkable transformation of China's financial landscape, from its nascent beginnings to a state of maturity and sophistication.

Initially piloted in China in 1992, Treasury bond futures faced significant challenges due to an immature market environment. Regrettably, incidents such as the notorious “319” and “327” manipulations led to the suspension of trading in 1995. At that time, the futures were tied to a single specific Treasury bond, with limited issuance volumes rendering the market susceptible to manipulation by large funds, fostering an environment conducive to irregularities.

After two decades of meticulous market nurturing and relentless enhancement of the regulatory regime, China's Treasury bond futures market was reinvigorated in 2013, amidst the maturing financial markets and deepening interest rate liberalization reforms. Since then, a diverse range of futures contracts—spanning 5-year, 10-year, 2-year, and 30-year maturities—have been introduced. This new system moves beyond a single underlying bond, adopting a nominal standard bond approach under which multiple eligible Treasury bonds serve as physical delivery assets. This effectively mitigates the risks of market manipulation.

Let's delve into the specifics of the 10-year Treasury bond future contract with code T2503, which will mature in March 2025. This contract commenced trading on June 17, 2024, and will conclude on March 14, 2025, the second Friday of the expiration month. Its nominal underlying is a 10-year Treasury bond issued on March 1, 2025, carrying a coupon rate of 3% and a face value of 1 million yuan. Eligible deliverable bonds must be interest-bearing Treasury bonds with maturities no longer than 10 years and remaining maturities of at least 6.5 years on March 1, 2025. As of February 19, 2025, according to the China Financial Futures Exchange's official website, there are 17 eligible bonds, with this number poised to grow with new issuances.

Given the abundance of deliverable bonds, the China Financial Futures Exchange (CFFEX) introduced the conversion factor (CF) as a vital tool to bridge the gap between nominal bond quotes and actual deliverable bond values. The final delivery amount is determined by the interplay of this conversion factor and the Treasury bond futures settlement price on the reporting date. For instance, assuming a settlement price of F, a

conversion factor of CF_i for bond i, and accrued interest AI_T^i at delivery time T, the formula for calculating the delivery amount for a 100-yuan face value contract is:

$$F \times CF_i + AI_T^i. \tag{1}$$

The CFFEX announces the conversion factor for each deliverable bond prior to futures listing, utilizing a complex formula that encompasses coupon rates, payment frequencies, and remaining payments. This formula ensures a fair and transparent valuation of the bonds for delivery purposes.

The specific formula is as follows:

$$\begin{aligned} CF = {} & \frac{\frac{c}{f}}{\left(1+\frac{r}{f}\right)^{f*\frac{x}{12}}} + \frac{\frac{c}{f}}{\left(1+\frac{r}{f}\right)^{f*\frac{x+\frac{12}{f}}{12}}} \\ & + \frac{\frac{c}{f}}{\left(1+\frac{r}{f}\right)^{f*\frac{x+2*\frac{12}{f}}{12}}} + \ldots + \frac{\left(\frac{c}{f}+1\right)}{\left(1+\frac{r}{f}\right)^{f*\frac{x+(n-1)*\frac{12}{f}}{12}}} \\ & - \frac{c}{f} \times \frac{12-fx}{12} = \frac{1}{(1+r/f)^{xf/12}} \\ & \left[\frac{c}{f} + \frac{c}{r}\left(1 - \frac{1}{(1+r/f)^{n-1}}\right) + \frac{1}{(1+r/f)^{n-1}}\right] \\ & - \frac{c}{f} \times \frac{12-fx}{12}. \end{aligned} \tag{2}$$

where

- $r = 3\%$, representing the discount rate used in the calculation.
- x denotes the number of months between the delivery month and the next interest payment month.
- n signifies the total number of remaining interest payments.
- c is the coupon of the deliverable bonds.
- f represents the frequency of interest payments per year for the deliverable bonds.

This formula meticulously discounts each coupon payment and the final principal repayment to their present values, using the given discount rate r. The sum of these discounted values, adjusted for the time elapsed since the last coupon payment, yields the conversion factor (CF). This factor is crucial in determining the relative value of different deliverable bonds for the purpose of futures contract delivery.

In addition, China employs the "Short Position Delivery Selection System" for Treasury bond futures deliveries. This system grants short sellers flexibility in choosing the delivery date and bonds, within a specified window from the first trading day of the expiration month to the second Friday. The conversion factor, based on a 3% market interest rate assumption, influences the attractiveness of bonds at delivery, fostering the concept of the cheapest to deliver (CTD) bond. Researchers have categorized the options held by short sellers into three types: quality options, rolling timing options, and month-end timing options, with the latter two collectively known as timing options, each characterized by unique futures and execution timings.

First, the quality option affords the short seller the prerogative to cherry-pick specific bonds from the pool of deliverable bonds for settlement. The exercise window for this option opens on the initial business day of the expiration month and remains open daily until 9:00 a.m. to 11:30 a.m. and 1:00 p.m. to 3:15 p.m. until the second Friday of the month.

Secondly, the rolling timing option provides short sellers with ample flexibility to select the delivery time frame within the specified hours (9:00 a.m. to 11:30 a.m. and 1:00 p.m. to 3:15 p.m.) on any day between the first working day and the business day preceding the second Friday of the expiration month. Additionally, on the final trading day, the window narrows to encompass solely the morning session, allowing short sellers to choose their delivery time between 9:30 and 11:30 a.m.

Lastly, the month-end timing option operates between 1:30 p.m. and 3:15 p.m. on the last trading day. Since the settlement price is determined at 11:30 a.m. and the deadline for declaring delivery intentions is 3:15 p.m., short sellers can use the known settlement price to acquire the most favorable bonds from the spot market for delivery during the afternoon session.

3.2 | Integrated Option

The interaction of three embedded options within the Treasury bond futures market—quality options, rolling timing options, and month-end timing options—forms an interdependent system where each factor significantly influences the others. The execution of these options follows a precise sequence and exhibits clear interdependence. Specifically, the enactment of quality options often coincides with the simultaneous activation of certain timing options, while rolling timing options and month-end timing options adhere to a distinct temporal hierarchy of effectiveness. Notably, the execution of rolling timing options can directly invalidate month-end timing options unless the short position voluntarily waives the former. This mutual constraint, along with potential cross-effects in rolling timing options, limits these three embedded options to a single execution window.

The complexity of this mechanism poses significant challenges for pricing Treasury bond futures, requiring market participants to analyze each option's characteristics thoroughly to develop a robust pricing strategy. Notably, in China's Treasury bond futures market, these embedded options tend to favor the short position, prompting the long position to price in these advantages to mitigate risks.

Market participants must understand the relationships between options to accurately assess their cumulative impact on Treasury bond futures pricing.

To address this, Yang (2025, working paper) have innovatively framed these three options as a single American-style option with multiple underlying assets, each featuring distinct strike prices. At the inception of the option, coinciding with the first business day of the futures' maturity month, the value of this integrated option is defined as follows:

$$O\left(F, T_0\right) = \sup_{\tau\in[T_0,T_1]} \mathrm{E}\left[\exp\left(-\int_{T_0}^{\tau} R_t dt\right) \max_{i=1:N}\left\{F \times \mathrm{CF}_i - P_{\tau i}^{\mathrm{clean}}\right\}\right]. \tag{3}$$

Here, E represents the real-world expectation, F is the Treasury bond futures price, T_0 and T_1 denote the start and end times of the three embedded options' lifespan, N is the count of deliverable bonds, $P_{\tau i}^{\mathrm{clean}}$ is the clean value of the ith asset at time τ, R_t is the discount rate corresponding to the volatility of the future, and CF_i is the conversion factor of the ith asset.

This option includes N underlying assets, each with a strike price of $F \times \mathrm{CF}_i$. During the interval $[T_0, T_1]$, the holder retains the right to exercise the option at any point. Notably, the payoff of this option may not be positive, as $\max_{i=1:\mathrm{N}}\left\{F \times \mathrm{CF}_i - P_{\tau i}^{\mathrm{clean}}\right\}$ can be negative, distinguishing it from traditional American options and earning it the designation of an "integrated option." In pricing Treasury bond futures, the goal is to find the optimal F where the value of this integrated option equals zero, balancing the interests of both long and short positions.

Furthermore, given the brevity of the interval $[T_0, T_1]$, and acknowledging the relatively low risk inherent in Treasury bond futures, Yang (2025, working paper) have refined the model into a more intuitive and computationally efficient format, tailored for practical real-world applications, as illustrated in Equation 4:

$$F^* = \arg\left\{O'(F, T_0) = \sup_{\tau\in[T_0,T_1]} \mathrm{E}\left[\mathrm{e}^{-r_0(\tau-T_0)} \max_{i=1:N}\left\{F \times CF_i - P_{\tau i}^{\mathrm{clean}}\right\}\right] = 0\right\}. \tag{4}$$

Here, F^* is the Treasury bond futures price that renders $O'(F, T_0) = 0$, and r_0 is the risk-free interest rate on the valuation date.

3.3 | "Valuation Deviations" and Generalized Error Distribution

The future clean price $P_{\tau i}^{\mathrm{clean}}$ corresponding to deliverable bond i and time τ is a stochastic variable, primarily influenced by shifts in market interest rates. Given the bond market's transparency and efficiency, bond prices converge daily towards valuations provided by official or third-party agencies. In China, the key third-party bond valuation institutions include ChinaBond Valuation (CCDC), ChinaSecurities Valuation (CSDS), CFETS Valuation (CFETS), and Shanghai Clearing House Valuation, each playing a pivotal role in the bond market.

Currently, the majority of investment institutions favor ChinaBond Valuation and ChinaSecurities Valuation as their benchmark references. ChinaBond Valuation serves as the cornerstone for bond trading and risk monitoring in the interbank market, exerting a broad influence. Conversely, ChinaSecurities Valuation offers a more comprehensive basis for assessing the valuation of exchange-traded bonds.

The ChinaBond Valuation System calculates clean prices by excluding accrued interest from the bond's full price, primarily for bond price evaluation and risk management. In line with industry standards, third-party valuation institutions, including ChinaBond Valuation, utilize valuation methodologies rooted in market yield curves. At the heart of this approach lies the cash flow discount model, which incorporates market information such as the China Bond yield curve and meticulously considers factors like the bond's remaining maturity, coupon rate, and credit rating.

In Treasury bond valuation, ChinaBond Valuation uses a unique yield curve developed by CCDC for Treasury bonds, combined with Hermite interpolation techniques. This methodology allows us to determine the yield to maturity for every bond. Subsequently, we discount all future cash flows based on this derived yield, ultimately arriving at the present value—which we term as the ChinaBond Valuation of the Treasury bond. The methodology employed in this process is outlined in the following steps:

Hermite interpolation: Suppose there are n key time points on a yield curve provided by CDCC, $0 \le t_1 < ... < t_i < ... < t_n \le T$, with corresponding yields $y_1, ..., y_i, ..., y_n$. Then, Equation (5), which is the cubic Hermite polynomial interpolation model, uses the three interest rates corresponding to t_{i-1}, t_i, and t_{i+1}, calculates the yield to maturity of $y(t)$ corresponding to any time point t (suppose $t_i < t < t_{i+1}$).

$$y(t) = y_i H_1 + y_{i+1} H_2 + d_i H_3 + d_{i+1} H_4. \tag{5}$$

In which,

$$H_1 = 3\left(\frac{t_{i+1}-t}{t_{i+1}-t_i}\right)^2 - 2\left(\frac{t_{i+1}-t}{t_{i+1}-t_i}\right)^3,$$
$$H_2 = 3\left(\frac{t-t_i}{t_{i+1}-t_i}\right)^2 - 2\left(\frac{t-t_i}{t_{i+1}-t_i}\right)^3,$$
$$H_3 = \frac{(t_{i+1}-t)^2}{t_{i+1}-t_i} - \frac{(t_{i+1}-t)^3}{(t_{i+1}-t_i)^2},$$
$$H_4 = \frac{(t-t_i)^3}{(t_{i+1}-t_i)^2} - \frac{(t-t_i)^2}{t_{i+1}-t_i},$$
$$d_i = \frac{dy(t_i)}{dt}, d_{i+1} = \frac{dy(t_{i+1})}{dt}.$$ [2]

ChinaBond Valuation: Equation (6) calculates the value of a t-year Treasury bond on the valuation date, based on the bond valuation model published by CCDC.

$$\mathrm{PV} = \frac{C/f}{(1+y/f)^w} + \frac{C/f}{(1+y/f)^{w+1}} + ... + \frac{\frac{C}{f}}{\left(1+\frac{y}{f}\right)^{w+N-1}} + \frac{FV}{\left(1+\frac{y}{f}\right)^{w+N-1}}, \tag{6}$$

where PV indicates the dirty price of the bond, y is the yield to maturity corresponding to this bond, C stands for the annual coupon payment, f represents the frequency of coupon payments per year, N denotes the number of remaining cash flows, FV is the Face value, $w = \frac{\mathrm{Day}}{\mathrm{Day}_0}$ indicates the next coupon time, Day represents the number of days between the valuation date and the next coupon payment date (including the first day but excluding the final day), and Day_0 denotes

the number of days between the last coupon date and the next coupon date.

ChinaBond Forward Valuation: Equation (4) focus on the projected future clean price of each deliverable bond, denoted as $P_{\tau i}^{\text{clean}}$. This clean price, excluding accrued interest, is influenced by various factors and fluctuates around its forward valuation. To estimate the ith bond's forward clean price, denoted as $P_{\tau i}^{\text{Est}}$, at the future time point τ, we employ the following formula:

$$P_{\tau i}^{\text{Est}} = \left(P_{0i}^{\text{full}} - D\right)(1 + y'/f)^{\tau * f} - \text{AI}_{\tau}. \tag{7}$$

In this equation:

- P_{0i}^{full} stands for the estimated bond value on the valuation date, derived from Equation (6).
- $P_{\tau i}^{\text{Est}}$ indicates the forward clean bond value corresponding to the future delivery date.
- τ is the time elapsed between the valuation date and the forward delivery date, calculated by dividing the number of days by 365.
- AI_{τ} denotes the Accrued interest at time τ.
- y' represents the yield to maturity corresponding time τ.

Furthermore, D signifies the present value of all coupon payments made on the bond during the period between the valuation date and the forward delivery date. It is calculated by summing up the present values of individual coupon payments, each discounted at rate y'. The calculation of D is given by the following formula:

$$\begin{aligned} D = &\frac{C/f}{(1 + y'/f)^{w}} + \frac{C/f}{(1 + y'/f)^{w+1}} \\ &+ \ldots + \frac{C/f}{(1 + y'/f)^{w+l-1}}, \end{aligned} \tag{8}$$

where l denotes the number of remaining cash flows between the valuation date and the forward delivery date.

The cornerstone of ChinaBond Valuation lies in its precise computation of prevailing market yields, serving as a benchmark for determining the fair value of Treasury bonds. Its objective is to mirror the theoretical worth of these bonds, devoid of any market distortions. Nevertheless, in the realm of actual transactions, the price of Treasury bonds undergoes dynamic shifts influenced by a myriad of market forces. These encompass, but are not limited to, intricate balances in supply and demand dynamics and fluctuations in investor sentiment. These intricate factors interact, causing the actual transaction price to oscillate around the fair value axis established by ChinaBond valuation framework.

Taking the deliverable bond i in a Treasury bond futures contract as an illustrative example, its projected future clean price is denoted as $P_{\tau i}^{\text{clean}}$. Meanwhile, the forward valuation $P_{\tau i}^{\text{Est}}$ offered by ChinaBond serves as a crucial reference point. To measure the discrepancy between these two values, we introduce the variable $X_{\tau i}^{\text{clean}-\text{Est}}$ defined as $P_{\tau i}^{\text{clean}} - P_{\tau i}^{\text{Est}}$, which represents the difference between the projected future clean price and the forward estimate of the clean price provided by ChinaBond.

Empirical research by Yang (2025, working paper) shows that the divergence between the actual clean price of each deliverable bond and ChinaBond's estimated clean price, termed "valuation deviations," follows a generalized error distribution. This revelation not only enhances our comprehension of the intricate nature of market pricing dynamics but also furnishes invaluable insights for subsequent endeavors in risk management, optimization of investment strategies, and market regulation.

The generalized error distribution, alternatively referred to as the Exponential Power Distribution, embodies remarkable flexibility as a continuous distribution function, capable of encompassing various significant distribution types as particular instances. Among these instances are the well-known normal distribution, the Laplace distribution, and any continuous uniform distribution confined within bounded intervals on the real number line. Thanks to its comprehensive coverage, the GED distribution has demonstrated exceptional versatility and applicability in practical contexts.

The generalized error distribution is characterized by three fundamental parameters: $\mu \in \mathrm{R}$, the location parameter, which designates the central position of the distribution; $\beta > 0$, the shape parameter, influencing the curvature or form of the distribution; and $\alpha > 0$, the scale parameter, regulating the degree of dispersion or the scaling factor of the distribution. This distribution is denoted as $\text{GED}(\mu, \alpha, \beta)$.

The probability density function (PDF) of the GED is given by the following equation:

$$f(x) = \frac{\beta}{2\alpha\Gamma(1/\beta)} e^{-(|x-\mu|/\alpha)^{\beta}}. \tag{9}$$

Here, $\Gamma(z)$ represents the gamma function, defined as:

$$\Gamma(z) = \int_0^{\infty} t^{z-1} e^{-t} dt. \tag{10}$$

The cumulative distribution function (CDF) of the GED is expressed as:

$$F(x) = \frac{1}{2} + \text{sign}(x - \mu)\frac{1}{2}\gamma\left(\frac{1}{\beta}, \left(\frac{|x - \mu|}{\alpha}\right)^{\beta}\right), \tag{11}$$

where $\gamma(z, x)$ is the lower incomplete gamma function, defined as:

$$\gamma(z, x) = \frac{1}{\Gamma(z)} \int_0^{x} t^{z-1} e^{-t} dt. \tag{12}$$

The mean of the $\text{GED}(\mu, \alpha, \beta)$ is μ, while its variance is given by $\frac{\alpha^2\Gamma(3/\beta)}{\Gamma(1/\beta)}$. The quantile function, which maps a probability p to the corresponding value x such that $F(x) = p$, can be expressed as follows:

$$F^{-1}(p) = \text{sign}(p - 0.5) \cdot \alpha \cdot \left[\gamma^{-1}\left(\frac{1}{\beta}, 2|p - 0.5|\right)\right]^{\frac{1}{\beta}} + \mu. \tag{13}$$

The GED exhibits interesting special cases based on the value of β:

- When $\beta = 2$, the generalized error distribution simplifies to the normal distribution with mean μ and variance $\alpha^2/2$. This reflects the fact that the normal distribution is a special case of the GED.
- When $\beta = 1$, the GED reduces to the Laplace distribution. The Laplace distribution has a sharp peak at its mean and relatively long tails, making it suitable for modeling data with outliers.
- As β approaches infinity ($\beta \to \infty$), the GED converges pointwise to a uniform distribution on the interval $(\mu - \alpha, \mu + \alpha)$. This means that for very large values of β, the GED becomes more and more uniform across this interval.

These special cases illustrate the flexibility of the GED in modeling various types of data distributions.

This distribution can be characterized by its shape parameter β, which distinguishes between two distinct behaviors in the data: a leptokurtosis and fat-tailed characteristic when $\beta < 2$, indicating a higher likelihood of extreme deviations, and a platykurtosis and thin-tailed when $\beta > 2$, suggesting a more evenly distributed set of deviations. In their working paper (Yang 2025), the authors observed that the "valuation deviation" exhibits a leptokurtosis and fat-tailed phenomenon, prompting them to conclude that the generalized error distribution captures this bias more precisely than the normal distribution. As a result, this finding holds significant potential for application in the pricing process of Treasury bond futures, enabling a more accurate estimation of the future valuation of each deliverable bond based on the yield curve at the pricing date.

In their paper, the authors assume that the future "valuation deviation" of each deliverable bond follows an independent and identically distributed GED model. This deviation is then added to the estimated valuation to represent the true clean price of the future deliverable bond. Utilizing the Monte Carlo simulation method, they simulate the future clean price of each deliverable bond. Based on these simulations, they determine the final deliverable bond values for the Treasury bond futures and establish the corresponding futures price. Under these assumptions, the model can be redefined as follows:

$$F^* = \arg\left\{ O'(F, T_0) = \sup_{\tau \in [T_0, T_1]} \mathrm{E}\left[\mathrm{e}^{-r_0(\tau - T_0)} \max_{i=1:N} \left\{ F \times CF_i - P_{\tau i}^{\mathrm{Est}} - X_{\tau i}^{\mathrm{clean-Est}} \right\} \right] = 0 \right\}. \tag{14}$$

In the above formula, $P_{\tau i}^{\mathrm{Est}}$ can be derived from the formula (7), and F is a constant. Consequently, the sole uncertain term that requires determination within this model is $X_{\tau i}^{\mathrm{clean-Est}}$.

3.4 | The Application of Copula Function in Treasury Bond Futures

Building on the research by Yang (2025, working paper), we refine and extend a key hypothesis in their study. In their original work, the authors assume that the differences between the anticipated clean prices of individual deliverable Treasury bonds and their forward valuations in ChinaBond, denoted as $\left\{ X_{\tau i}^{\mathrm{clean-Est}} \right\}_{i=1:N}$, follow an independent and identically distributed generalized error distribution. They use Monte Carlo simulation to numerically solve model (14). To better capture market dynamics, especially the interactions among deliverable bonds, we propose an enhanced framework.

We posit that these discrepancies not only follow GEDs, but also exhibit a nuanced correlation structure. To meticulously capture this interdependence, we harness the versatile Copula function as a powerful analytical lens.

The Copula function connects the marginal distributions of multiple random variables to their joint distribution. Its key strength is separating the dependence structure from the marginal distributions, providing flexibility in analysis. Key features of the Copula approach include:

- Flexibility: It combines diverse marginal distributions with complex dependency structures to create multivariate models.
- Non-parametric Nature: It does not rely on specific distributional forms, accommodating non-linear and non-normal dependencies.
- Universal Application: It is widely used in finance, environmental science, and hydrology.
- Diversity of Forms: Many kinds of Copulas, such as Gaussian Copula, Student's t-Copula, Frank Copula, Gumbel Copula, and Clayton Copula, capture distinct dependency patterns.

Rooted in Gaussian distribution, the Gaussian Copula models' symmetric dependencies easily, with simple computation and broad applicability in asset portfolio management and derivatives pricing. The Gaussian Copula's formulation is grounded in the CDF of the standard normal distribution, ϕ, and its inverse, ϕ^{-1}. For N random variables, the Gaussian Copula function, C, is expressed as:

$$C_{\mathrm{Gaussian}}(v_1, v_2, ..., v_N; \rho) = \phi_\rho(\phi^{-1}(v_1), \phi^{-1}(v_2), ..., \phi^{-1}(v_N)), \tag{15}$$

where ϕ_ρ represents the CDF of the N-dimensional normal distribution with correlation coefficient matrix ρ.

The Student's t-Copula incorporates heavier tails through its degrees of freedom parameter ν. Its multivariate t-distribution foundation captures extreme co-movements, making it particularly valuable in risk management during market crises. The Student's t-Copula is defined as:

$$C_{\mathrm{Student}}(v_1, v_2, ..., v_N; \rho, \nu) = t_{\rho,\nu}\left(t_\nu^{-1}(v_1), t_\nu^{-1}(v_2), ..., t_\nu^{-1}(v_N) \right), \tag{16}$$

where $t_\nu(\bullet)$ denotes the univariate t-distribution CDF with ν degrees of freedom.

The Clayton Copula model's asymmetric dependence, particularly lower tail dependence, through its parameter $\theta > 0$. Frequently applied in insurance and default risk analysis, it emphasizes joint extreme negative events. Its generator function $\varphi(t) = (t^{-\theta} - 1)/\theta$ yields the closed-form expression:

$$C_{\text{Clayton}}(v_1, v_2, ..., v_N; \theta) = \left(\sum_{i=1}^{N} v_i^{-\theta} - N + 1\right)^{-1/\theta}. \quad (17)$$

The Gumbel Copula models upper tail dependence with parameter $\theta \geq 1$. Its structure $\varphi(t) = (-\ln t)^{\theta}$ proves effective in modeling joint maxima phenomena, particularly in environmental extremes and catastrophe bonds. The Archimedean formulation becomes:

$$C_{\text{Gumbel}}(v_1, v_2, ..., v_N; \theta) = \exp\left(-\sum_{i=1}^{N} (-\ln v_i)^{\theta}\right)^{1/\theta}. \quad (18)$$

The Frank Copula provides symmetric dependence without tail concentration through parameter $\theta \neq 0$. Its generator $\varphi(t) = -\ln \frac{\exp(-\theta t) - 1}{\exp(-\theta) - 1}$ facilitates dependence modeling in credit derivatives and hydrological studies:

$$C_{\text{Frank}}(v_1, v_2, ..., v_N; \theta) = -\frac{1}{\theta} \ln\left(1 + \frac{\prod_{i=1}^{N}(\exp(-\theta v_i) - 1)}{(\exp(-\theta) - 1)^{N-1}}\right). \quad (19)$$

This variety of Copulas allows practitioners to choose dependency structures that match their needs, such as tail sensitivity (Clayton/Gumbel), symmetric heavy tails (Student's t), or parametric flexibility (Frank).

In this study, we integrate these Copulas with the GED marginal distributions of the "valuation deviations" $\left\{X_{\tau i}^{\text{clean}-\text{Est}}\right\}_{i=1:N}$ for deliverable bonds in Treasury bond futures, constructing a joint distribution model that better reflects real-world market conditions. This integration allows us to model the intricate correlation structures within the system:

$$\Pr\left(X_{\tau 1}^{\text{clean}-\text{Est}} \leq x_1, X_{\tau 2}^{\text{clean}-\text{Est}} \leq x_2, ..., X_{\tau n}^{\text{clean}-\text{Est}} \leq x_N\right) = C\left(F_{\tau}^{1}(x_1), F_{\tau}^{2}(x_2), ..., F_{\tau}^{n}(x_N)\right), \quad (20)$$

where the parameters of the GED distributions and the Copulas are empirically derived from historical bond data and $C(\bullet, \bullet, ..., \bullet)$ is one of the Copulas mentioned.

Critically, the GED-Copula framework proposed here aims to characterize statistical regularities arising from coordinated institutional behavior under China's policy constraints—such as collective trading triggered by window guidance or liquidity comovement under capital controls—rather than stochastic price discovery in fully liberalized markets. This theoretical positioning originates from the institutional features detailed in Section 1: state-owned institutions holding > 63% of positions, the exclusive control granted to short positions by delivery rules, and normalized policy interventions collectively shape the heavy-tailed dependence in valuation deviations.

Under this refined framework, we redesign the pricing strategy for Treasury bond futures. First, we estimate the GED distribution parameters and their correlation matrix using historical data. Next, we use Copulas to combine these marginal distributions into a joint distribution. Finally, we apply Monte Carlo simulation to sample from this joint distribution and numerically solve model (14), providing more accurate and robust pricing estimates for Treasury bond futures.

3.5 | Pricing Steps for Treasury Bond Futures

Given the intricacies of the joint distribution calculations within model (16), we adopt numerical methods to price Treasury bond futures in model (14), avoiding the difficulty of deriving explicit solutions directly. The comprehensive pricing process involves the following steps:

Data Collection and Processing: For each eligible deliverable bond, we gather its historical ChinaBond valuation data and corresponding closing price data. The difference between these two datasets is then computed and used to form a comprehensive sample set to capture historical valuation deviations.

GED Parameter Estimation: Using the collected historical data, we employ the least squares method to estimate the parameter set $\{\mu_i, \alpha_i, \beta_i\}_{i=1:N}$ of the generalized error distribution for each deliverable bond's valuation deviation.

Copulas Parameter Estimation: We select the contemporaneous observational data of all deliverable bonds to construct a common panel dataset. Based on the GED parameter estimation results from the previous step, we calculate the CDF values at each time point through probability integral transformation, generating a uniform distribution probability matrix $U = [u_{1t}, u_{2t}, ..., u_{Nt}]_{t=1:T}$ with dimensions equal to the number of deliverable bonds.

Using the aforementioned probability matrix U as the empirical joint distribution input, estimate the parameters of the target Copula function through the maximum likelihood method:

Gaussian: Estimate the correlation coefficient matrix ρ;

Student's t: Estimate the correlation coefficient matrix ρ and degrees of freedom ν;

Clayton/Gumbel/Frank: Estimate the tail dependence parameter θ.

Random Number Generation: For each Copula, and for each deliverable bond n (where n ranges from 1 to N), we use Equation (13) to calculate the quantile of the GED distribution corresponding to the random numbers $\{u_{m,n,t}\}$ for all m and t values, using the bond-specific parameters $\{\mu_n, \alpha_n, \beta_n\}$. These quantiles form a three-dimensional random number array X of valuation deviations, with elements $x_{m,n,t}$ for $m = 1:M$, $n = 1:N$, and $t = 1:T$.

GED Quantile Calculation: For each Copula, and for each deliverable bond n (ranging from 1 to N), we use Equation (13) to calculate the GED distribution quantile corresponding to the random numbers $\{u_{m,n,t}\}$ for all m and t values, using the bond-specific parameters $\{\mu_n, \alpha_n, \beta_n\}$. These quantiles form a three-dimensional random number array X of valuation deviations, with elements $x_{m,n,t}$ for $m = 1:M$, $n = 1:N$, and $t = 1:T$.

ChinaBond Forward Valuation: Using the current market yield curve and bond terms, we compute the Forward Valuation of ChinaBond for each deliverable bond on each future delivery date using Equation (7).

Model Solving: Finally, we incorporate the valuation deviation random number matrix X and the ChinaBond Forward

Valuations into model (14). Using iterative and optimization algorithms, we adjust the variable F until the embedded option value within the model converges to zero. After several iterations, we arrive at a reasonable price for the Treasury bond futures, which serves as the final result.

4 | Empirical Analysis of Treasury Bond Futures

4.1 | The Data of Treasury Bond Futures

We have chosen T2503 Treasury bond futures as the focus of our research. This futures contract is scheduled to commence trading on June 17, 2024, and will expire on March 14, 2025. Holders of short positions in Treasury bond futures have the option to deliver their positions on any business day between March 3 and March 14, 2025. The theoretical underlying asset for T2503 Treasury bond futures is a 10-year Treasury bond, set to be issued on March 1, 2025, offering a coupon rate of 3% with semi-annual interest payments.

Our research sample comprises all closing price data for T2503 Treasury bond futures, spanning from its listing date to February 19, 2025, as depicted in Figure 1. A cursory glance at the chart reveals a predominantly upward trend in the futures prices during the selected timeframe, reflecting market expectations of declining interest rates. Nevertheless, it is notable that prices underwent a notable correction in the final few days, potentially signaling a subtle shift in market sentiment regarding future monetary policy or an initial response to looming economic uncertainties.

To gain a deeper understanding of the price fluctuation patterns of T2503 Treasury bond futures during this period, we have compiled and analyzed relevant statistical data, summarized in Table 1. The data reveals that the volatility of this futures contract is relatively low, underscoring the stability of its price movements. The skewness value of 0.5006 hints at a possible right-skewed price distribution. Meanwhile, the excess kurtosis of −1.1173 indicates a flatter tail in the price distribution compared to a normal distribution, suggesting a lower frequency of extreme values. This observation reinforces the notion of stable price fluctuations in T2503 Treasury bond futures, consistent with the widely held belief that Treasury bonds represent low-risk investment options.

4.2 | Information on T2503 Deliverable Bonds

As of February 19, 2025, a total of 17 eligible deliverable bonds have been identified under the T2503 contract for Treasury bond futures. The comprehensive details of these bonds are summarized in Table 2 below.

We have compiled the historical closing prices (in clean price format) of these 17 deliverable bonds, along with their corresponding ChinaBond valuation data. Our objective is to calculate the valuation deviations for each bond. Recognizing that these deliverable bonds have different listing dates, resulting in varying historical sample sizes, we have organized and presented the relevant data systematically in Table 3. This ensures that readers gain a clear and comprehensive understanding of the valuation deviations for each individual bond.

Upon examining the data presented in the table above, it becomes evident that each valuation deviation exhibits a high level of kurtosis, signifying that the data distribution possesses distinct leptokurtic and fat-tailed characteristic. The skewness exhibits a mixed pattern, encompassing both positive and negative values, and lacks overall consistency. Given the non-normal characteristics of this distribution, employing the generalized error distribution as a modeling tool to depict these valuation deviations is a highly appropriate and rational decision. Renowned for its versatility and adaptability, the GED distribution adeptly captures and delineates various non-

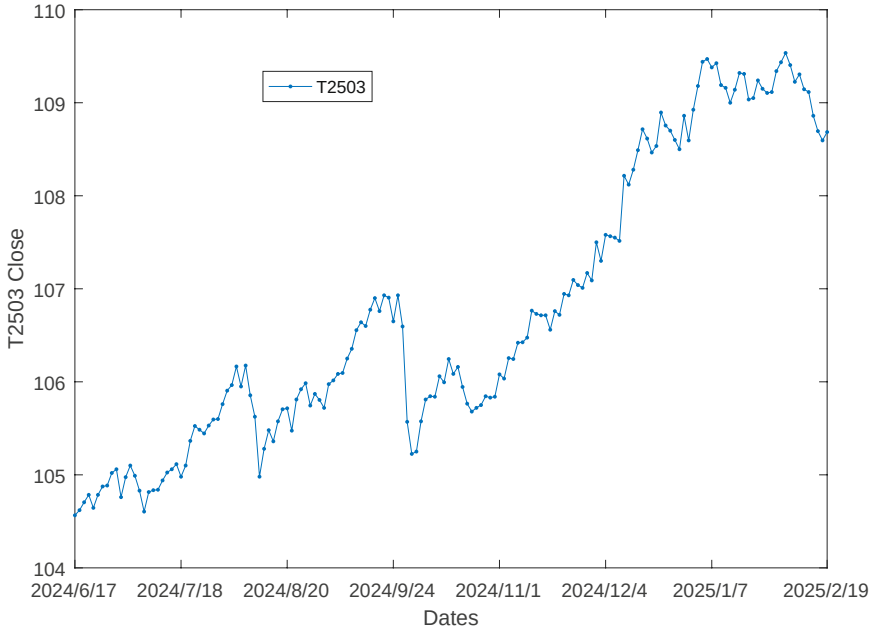

FIGURE 1 | Trend of T2503 closing prices. [Color figure can be viewed at wileyonlinelibrary.com]

TABLE 1 | T2503 treasury bond futures historical closing prices statistics.

Sample no.	Mean	SD	Max	Min	Skew.	Ex-Kurt.
164	106.7551	1.5249	109.535	104.5650	0.5006	−1.1173

TABLE 2 | Details of T2503 deliverable bonds.

No.	Code	Issue	Mat.	Freq.	Coupon(%)	CF
1	240018	2024/9/15	2031/9/15	1	1.87	0.9341
2	210017	2021/11/18	2031/11/18	2	2.89	0.9934
3	240025	2024/12/25	2031/12/25	1	1.49	0.9089
4	220003	2022/02/17	2032/2/17	2	2.75	0.9845
5	220010	2022/5/15	2032/5/15	2	2.76	0.9846
6	220017	2022/8/15	2032/8/15	2	2.69	0.9795
7	220025	2022/11/15	2032/11/15	2	2.8	0.9864
8	230004	2023/2/25	2033/2/25	2	2.88	0.9916
9	230012	2023/5/25	2033/5/25	2	2.67	0.9762
10	230018	2023/8/25	2033/8/25	2	2.52	0.9645
11	230026	2023/11/25	2033/11/25	2	2.67	0.975
12	240004	2024/2/25	2034/2/25	2	2.35	0.9495
13	240011	2024/5/25	2034/5/25	2	2.27	0.9419
14	240017	2024/8/25	2034/8/25	2	2.11	0.9274
15	2400101	2024/8/29	2034/8/29	2	2.17	0.9323
16	240023	2024/11/25	2034/11/25	2	2.06	0.9199
17	250004	2025/2/15	2035/2/15	2	1.61	0.8815

TABLE 3 | Details of historical valuation deviations for T2503 deliverable bonds.

No.	Sample start[a]	Sample end	Sample no.	Mean	SD	Max	Min.	Skew.	Ex-Kurt.
1	2024/09/20	2025/2/19	101	0.0082	0.1308	0.7381	−0.4322	2.6897	15.6474
2	2021/11/22		811	−0.0041	0.0978	1.1187	−0.5479	2.9555	32.7053
3	2024/12/27		34	−0.0027	0.0683	0.1605	−0.1479	−0.1898	0.1619
4	2022/2/21		705	−0.0004	0.1007	1.5921	−0.7766	5.5966	96.7209
5	2022/5/18		690	−0.0084	0.1019	1.4201	−0.5058	4.9713	65.8569
6	2022/8/17		626	−0.0086	0.1439	1.6692	−1.2789	1.2045	56.4649
7	2022/11/17		564	−0.0038	0.1025	0.7223	−0.6678	1.1974	15.9822
8	2023/3/1		493	−0.0061	0.1148	1.5944	−0.4212	5.8598	80.3899
9	2023/5/30		432	−0.0153	0.1254	0.5158	−1.9746	−8.8389	137.7917
10	2023/8/29		367	−0.0135	0.0936	0.4901	−0.7736	−0.9548	15.4697
11	2023/11/29		305	−0.0067	0.0902	0.5820	−0.3603	1.9011	14.2141
12	2024/2/28		244	−0.0084	0.1045	0.4166	−0.4109	−0.2722	3.9099
13	2024/5/29		181	−0.0078	0.0932	0.5386	−0.4575	0.3669	9.7452
14	2024/08/28		117	0.0139	0.1460	1.2801	−0.2877	5.5005	47.0079
15	2024/8/29		116	−0.0232	0.1438	0.4018	−0.9073	−2.0978	12.1859
16	2024/11/27		56	−0.0129	0.1341	0.2783	−0.5588	−1.2315	4.0070
17	2025/2/19		1	−0.0688	NaN[b]	−0.0688	−0.0688	NaN	NaN

[a]The discrepancy between the sample start dates and the issuance dates of the bonds arises from the fact that the actual listing date of the bonds lags behind their issue date by two business days.
[b]With only one sample, it is not possible to calculate standard deviation, skewness and excess kurtosis.

normal traits, particularly leptokurtic and fat-tailed characteristics, thereby providing a more precise and exhaustive analysis of valuation deviations.

4.3 | Information on Treasury Yield to Maturity Curve

In the process of simulating Treasury bond prices, meticulously calculating the ChinaBond forward valuation is a critical step. To ensure the accuracy and robustness of our model, we have carefully collected the most comprehensive Treasury yield to maturity curve data, covering the period from June 17, 2024, to February 19, 2025, directly from the website of the China Bond Market Clearing Corporation (http://www.chinabond.com.cn).

As an example, let us examine the detailed yield to maturity curve as of June 17, 2024. Table 4 below presents the key yield to maturity points for various maturity terms, sourced directly from the China Bond Market Clearing Corporation's website. This information provides a snapshot of the market conditions on that date.

4.4 | Comprehensive Pricing Performance and Copula Model Comparison for the T2503 Contract

4.4.1 | Pricing Process Demonstration: A Case Study of June 17, 2024

The intricate process of pricing Treasury bond futures requires a rigorous and comprehensive methodology to ensure precision. To simplify, we focus exclusively on the pricing of Treasury bond futures under the Gaussian Copula framework. This section delves into each step of the pricing process, using June 17, 2024, as a concrete example, elucidating the detailed logic and computational steps.

Step 1: Estimating GED Distribution Parameters for Valuation Deviations of Deliverable Bonds

First, we collected all closing clean price data for each deliverable bond, spanning from their issuance dates to June 17, 2024. Simultaneously, we obtained corresponding ChinaBond Valuation data. By calculating the differences between these two datasets, we constructed a sample set to estimate the parameters of the generalized error distribution model.

For bonds with limited transaction records leading to insufficient sample sizes (e.g., less than 30 observations), we exclude them from our pricing framework to prevent potential distortions in subsequent Copula parameter estimation.

Employing the maximum likelihood estimation (MLE) method, we calibrated the GED parameters, as summarized in Table 5.

The beta values in Table 5, consistently below 2, underscore the GED model's effectiveness in capturing the leptokurtosis and fat-tailed characteristics of bond valuation deviations. This finding underpins our subsequent development and refinement of treasury bond futures pricing strategies leveraging the GED distribution.

Step 2: Calibration of Correlation Coefficient matrix ρ

We select the contemporaneous observational valuation deviations for all deliverable bonds to construct a common panel dataset. Using the GED model parameter estimation results obtained in the previous step, we calculate the CDF values for each bond's data. Subsequently, based on this entire panel of CDF values, proceed with the parameter calibration of the correlation coefficient matrix ρ for the Gaussian Copula. Table 6 presents the estimation results.

Notably, high-correlation pairs (e.g., Bonds 6–9: $\rho = 0.5966$) predominantly involve deliverable bonds held by state-owned commercial banks, suggesting synchronized trading under policy directives explains observed dependence. Low-correlation pairs (e.g., Bonds 2–11: $\rho = 0.1079$) often involve bonds traded by non-bank institutions with weaker policy sensitivity. This institutional clustering validates our model's theoretical grounding in policy-driven co-movements.

Step 3: Simulating and Projecting Future Valuation Deviations

To accurately simulate the anticipated fluctuations in valuation deviations across various future delivery dates for each deliverable bond, we have devised a meticulous methodology based on the correlation coefficient matrix outlined in Table 6.

TABLE 4 | Key yields of the yield to maturity curve on June 17, 2024.

Maturity (Year)	Yield (%)	Maturity (Year)	Yield (%)
0	1.318	5	2.0659
0.08	1.5105	7	2.2116
0.17	1.5198	10	2.2609
0.25	1.5376	15	2.3652
0.5	1.5724	20	2.4106
0.75	1.5896	30	2.5057
1	1.604	40	2.5422
2	1.7862	50	2.545
3	1.9109		

Source: China Bond Market Clearing Corporation (www.chinabond.com.cn)

TABLE 5 | Estimated GED parameters for deliverable bonds.

Bond No.[a]	μ	α	β
2	−0.0010	0.0066	0.4873
4	−0.0016	0.0141	0.6103
5	−0.0051	0.0087	0.5504
6	−0.0082	0.0046	0.4365
7	−0.0001	0.0034	0.4190
8	0.0000	0.0050	0.4641
9	−0.0166	0.0142	0.5838
10	−0.0047	0.0119	0.5872
11	−0.0014	0.0124	0.6105
12	−0.0127	0.0300	0.7482

[a]As of June 17, 2024, only 10 deliverable bonds from bond series 2, and 4 to 12 in Table 2 are available. However, the remaining six bonds have not yet been listed on the market, and one bond, although listed, has fewer than 30 trading days for historical data, rendering it insufficient for robust statistical analysis.

First, for each deliverable date, we generate $M = 100{,}000$ N-dimensional normal random number sequences. These sequences are carefully designed to ensure that their correlation coefficients precisely align with the specifications detailed in Table 6. By iteratively repeating this simulation T times and combing the resulting random number matrices across all delivery dates, we construct an expansive $M \times N \times T$ three-dimensional random matrix. In this matrix, M stands as a testament to the number of distinct simulation paths, N encapsulates the total count of deliverable bonds, and T represents the comprehensive tally of delivery dates.

Subsequently, to align these normally distributed random numbers with the inherent valuation deviation characteristics unique to each bond, we implement a tailored transformation process for each deliverable bond. This transformation leverages the bond's specific generalized error distribution parameters—comprising the mean (μ), shape (α), and scale (β), as detailed in Table 5—which collectively define the bond's distinct valuation deviation pattern.

At the heart of this transformation lies the utilization of the inverse cumulative distribution function (ICDF) of the GED distribution (as stipulated in Equation 13). This crucial step maps the normally distributed random numbers onto their corresponding GED distribution, resulting in a set of random numbers that more accurately reflect the actual valuation deviations experienced by the bonds. Table 7 offers a tangible illustration of this process, showcasing a representative sample of valuation deviation random numbers, vividly demonstrating the significant and random variations across bonds and delivery dates, mirroring market volatility and uncertainty.

Through this process, we have successfully constructed a simulated dataset that reflects future variations in valuation deviations, providing a solid foundation for subsequent pricing analysis of Treasury bond futures. These random numbers representing valuation deviations will be directly applied to Model (14) to calculate the reasonable prices of Treasury bond futures under different market conditions.

Step 4: Forward Valuation of Deliverable Bonds

We calculated the forward clean price (P_{ti}^{Est}) using formula (7) based on the yield to maturity curve of ChinaBond, as shown in Table 4, and summarized the results in Table 8. This table shows the estimated forward valuation of all deliverable bonds on June 17, 2024 for the future 10 deliverable dates.

Step 5: Final Futures Pricing

After determining the valuation deviations and forward valuations, we input critical data from Tables 7 and 8 into the

TABLE 6 | Correlation matrix of valuation deviations.

No.	2	4	5	6	7	8	9	10	11	12
2	1.0000	0.4761	0.3525	0.4507	0.3432	0.2906	0.3843	0.1540	0.1079	0.2849
4	0.4761	1.0000	0.2802	0.3922	0.2852	0.1484	0.2252	0.1926	0.3070	0.2914
5	0.3525	0.2802	1.0000	0.4313	0.4477	0.3886	0.3329	0.1096	0.1354	0.2905
6	0.4507	0.3922	0.4313	1.0000	0.3964	0.4004	0.5966	0.4547	0.1394	0.3297
7	0.3432	0.2852	0.4477	0.3964	1.0000	0.2810	0.1956	0.0241	0.1211	0.2610
8	0.2906	0.1484	0.3886	0.4004	0.2810	1.0000	0.3240	0.1844	0.0146	0.3641
9	0.3843	0.2252	0.3329	0.5966	0.1956	0.3240	1.0000	0.4976	−0.0269	0.3094
10	0.1540	0.1926	0.1096	0.4547	0.0241	0.1844	0.4976	1.0000	0.3687	0.2852
11	0.1079	0.3070	0.1354	0.1394	0.1211	0.0146	−0.0269	0.3687	1.0000	0.2137
12	0.2849	0.2914	0.2905	0.3297	0.2610	0.3641	0.3094	0.2852	0.2137	1.0000

TABLE 7 | Sample of simulated valuation deviations.

Date bond	1	2	3	4	5	6	7	8	9	10
2	−0.0168	−0.0427	0.0078	−0.0488	0.0175	−0.0017	0.0312	0.0021	0.0179	0.0344
4	−0.0589	−0.0010	−0.0515	−0.0191	0.0719	−0.0287	0.0311	0.0523	−0.0492	−0.0004
5	−0.0026	0.0190	0.0436	−0.0229	−0.0033	-0.0051	−0.0336	0.0483	0.0346	−0.0169
6	−0.0069	−0.0084	−0.0053	−0.0279	0.0226	-0.0339	0.0056	0.0538	0.0004	−0.0498
7	−0.0659	−0.0002	0.0467	0.0207	0.0929	0.0021	−0.0165	0.0874	0.0138	−0.0523
8	−0.0178	−0.0225	−0.0022	−0.1480	−0.0012	−0.0032	0.0323	0.0421	−0.0096	0.0034
9	0.0198	−0.0135	−0.0172	−0.0639	0.0079	−0.0236	−0.0468	0.1741	−0.0477	0.0538
10	0.1555	−0.0118	−0.0695	0.0073	0.0144	−0.0703	−0.0212	0.0711	−0.0455	−0.0056
11	−0.0007	0.0550	−0.1628	0.0008	0.0533	−0.0510	0.0015	0.0009	−0.0072	−0.1983
12	−0.0090	−0.0204	0.0227	−0.0623	0.0819	−0.0969	0.0062	0.0043	−0.0258	−0.0846

pre-established model (Equation 14). We used an iterative method to identify the Treasury bond futures price, F, that satisfies the condition $O'(F, T_0) = 0$. After several iterations, we derived a fair price for the Treasury bond futures, $F = 103.7069$, assuming a simulated path count of $M = 100{,}000$. However, when compared to the same day's closing price of the T2503 contract, 104.565, we observed a slight discrepancy. This deviation could stem from multifaceted factors, such as abrupt market sentiment shifts, the immediate impact of new market information, and dynamic fluctuations in market liquidity.

4.4.2 | Model Stability Evaluation

To assess the stability of our model, we conducted a case study using June 17, 2024. This involved altering the number of simulations (M) and replicating the pricing process 20 times for each value of M. Subsequently, we calculated the standard deviation of these pricing outcomes for each M, as depicted in Figure 2, to gain insights into the model's stability.

As evident from the figure, the standard deviation of Treasury bond futures prices exhibits a pronounced decline as the number of simulated paths increases from 200 to 102,400. This decrease is substantial, dropping from an initial value of 0.01 to a mere 0.00035. Given the fact that the smallest price tick for 10-year Treasury bond futures is 0.002, our model achieves remarkable precision when the number of simulated paths reaches 100,000. At this point, the standard deviation of the predicted prices becomes virtually negligible, remaining well within the 0.002 range, indicative of near-perfect accuracy.

Therefore, we confidently conclude that with at least of 100,000 simulated paths, our model can deliver highly stable predictions for Treasury bond futures prices, thereby providing financial decision-makers with a solid and highly reliable quantitative foundation.

TABLE 8 | Forward valuation of deliverable bonds.

Date bond	1	2	3	4	5	6	7	8	9	10
2	103.7737	103.7445	103.7916	103.7317	103.7947	103.7655	103.7951	103.7627	103.7751	103.7884
4	102.7005	102.7554	102.7020	102.7313	102.8193	102.7097	102.7665	102.7846	102.6801	102.7259
5	102.8073	102.8259	102.8475	102.7780	102.7946	102.7838	102.7522	102.8312	102.8144	102.7600
6	102.3454	102.3410	102.3412	102.3158	102.3635	102.2983	102.3350	102.3804	102.3241	102.2710
7	103.1346	103.1972	103.2410	103.2118	103.2810	103.1809	103.1592	103.2600	103.1833	103.1142
8	103.9125	103.9045	103.9215	103.7723	103.9158	103.9038	103.9361	103.9426	103.8875	103.8972
9	102.3000	102.2639	102.2573	102.2079	102.2769	102.2370	102.2111	102.4291	102.2046	102.3033
10	101.3417	101.1720	101.1119	101.1862	101.1909	101.0987	101.1454	101.2353	101.1162	101.1537
11	102.4106	102.4636	102.2429	102.4038	102.4535	102.3408	102.3906	102.3872	102.3764	102.1825
12	99.9982	99.9848	100.0258	99.9388	100.0810	99.8961	99.9971	99.9932	99.9610	99.9003

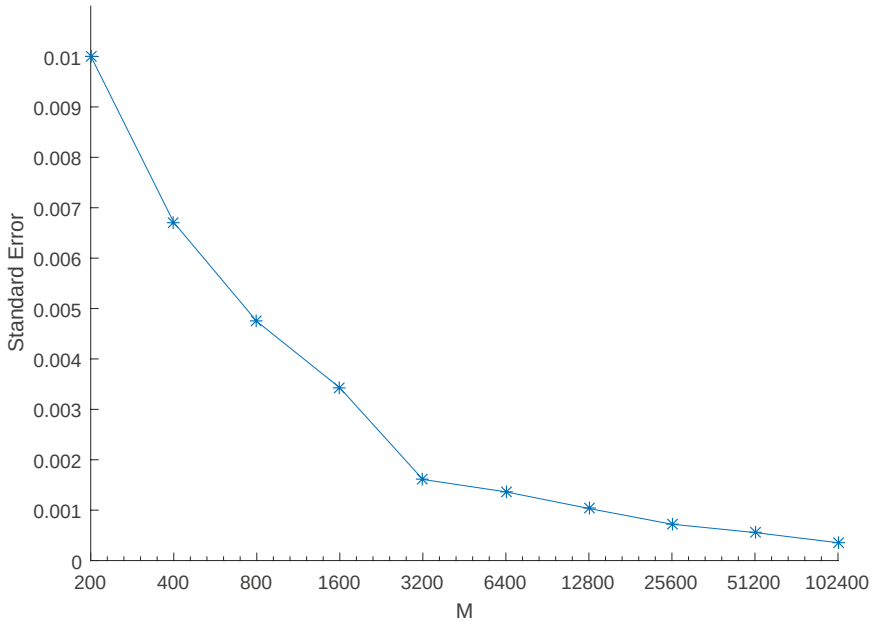

FIGURE 2 | Evolution of treasury bond futures price standard deviation with increasing number of simulated paths. [Color figure can be viewed at wileyonlinelibrary.com]

4.4.3 | *Overall Pricing Performance of the T2503 Contract and Analysis of Systematic Bias*

We applied the pricing model to the entire lifespan of the T2503 contract (June 17, 2024, to February 19, 2025). Figure 3 compares the model's daily prices (using the Student's *t*-Copula) with the actual closing prices. While a strong co-movement is evident, the model exhibits a systematic underestimation.

Table 9 (first row, Student's *t*) quantifies the pricing errors, which, while acceptable, confirm this systematic bias. We hypothesize that this stems from the model's insufficient incorporation of market sentiment during the pronounced rate-cutting cycle (Figure 4), which likely infused market prices with an "optimism premium."

To test this hypothesis, we priced the T2106 contract (Figure 5), which traded in a period without a strong unilateral rate trend. For T2106, the model prices fluctuate evenly around the market prices, showing no systematic bias. This contrast substantiates our hypothesis that the systematic deviation for T2503 is linked to the strong policy-driven market trend.

4.4.4 | *Performance Comparison of Copula-Based Models*

We compared the pricing performance of five different Copulas over the entire T2503 sample. The results are visualized in Figure 6 and quantified in Table 9. While performance is generally similar, the Student's t-Copula consistently achieves the lowest errors, attributable to its superior ability to model symmetric heavy-tailed dependence. The pricing paths of the Gumbel and Frank Copulas are nearly identical.

4.4.5 | *Comparison with the Nunes and Oliveira (2007) Model*

We benchmarked our best-performing model (Student's *t*-Copula) against the classical approach of Nunes and Oliveira (2007). As shown in Figure 7, while their model performs well on the strongly trending T2503 contract, its performance on the more volatile T2106 contract is less consistent. This suggests that their model, which is calibrated to market prices, may be better suited to stable, trending markets. In contrast, our model, which explicitly incorporates the yield curve dynamics, demonstrates greater robustness in a wider range of market conditions.

From a theoretical perspective, a key distinction lies in the treatment of embedded options. The Nunes and Oliveira (2007) framework focuses on the quality option, whereas our model provides an integrated valuation of both quality and timing options. It is worth noting that their calibration to market prices, which inherently include the value of all embedded options, introduces a potential limitation, as the calibrated parameters may implicitly subsume the value of omitted timing options.

4.5 | Policy-Driven Model Enhancement and Pricing Performance Improvement

As shown in Section 4.4-3, the original model exhibited systematic undervaluation during the sample period of the T2503 contract. We posit that this bias stems from the model's inability to fully capture the pricing impact of coordinated policy guidance. As

TABLE 9 | Discrepancy analysis: T2503 treasury bond futures closing prices versus predicted prices from different copula-based models.

Model	MSE	MAE	Max-AE	Min-AE
Gaussian	0.4276	0.6297	0.9987	0.0105
Student's *t*	0.2780	0.5064	0.8442	0.0167
Clayton	0.4408	0.6395	0.9862	0.0118
Gumbel	0.5116	0.6889	1.0116	0.0076
Frank	0.5137	0.6905	1.0125	0.0076

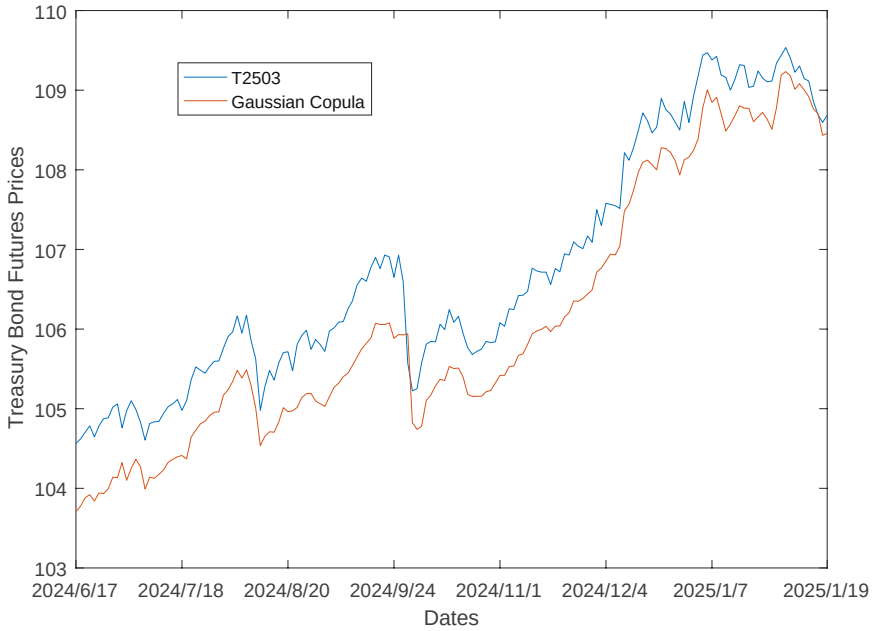

FIGURE 3 | Comparison of model pricing results and actual closing prices for T2503.

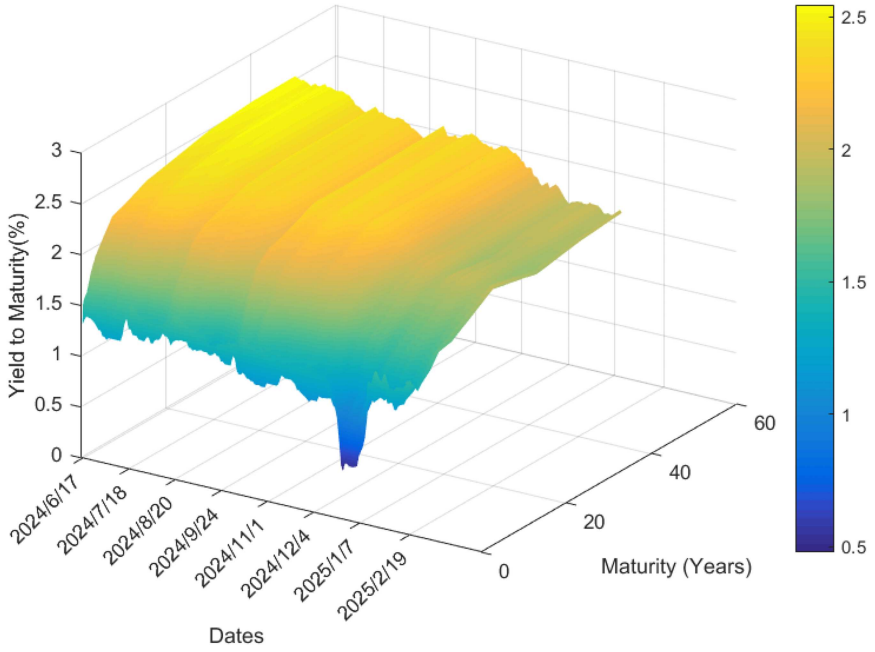

FIGURE 4 | Yield to maturity movement from June 17, 2024 to February 19, 2025. [Color figure can be viewed at wileyonlinelibrary.com]

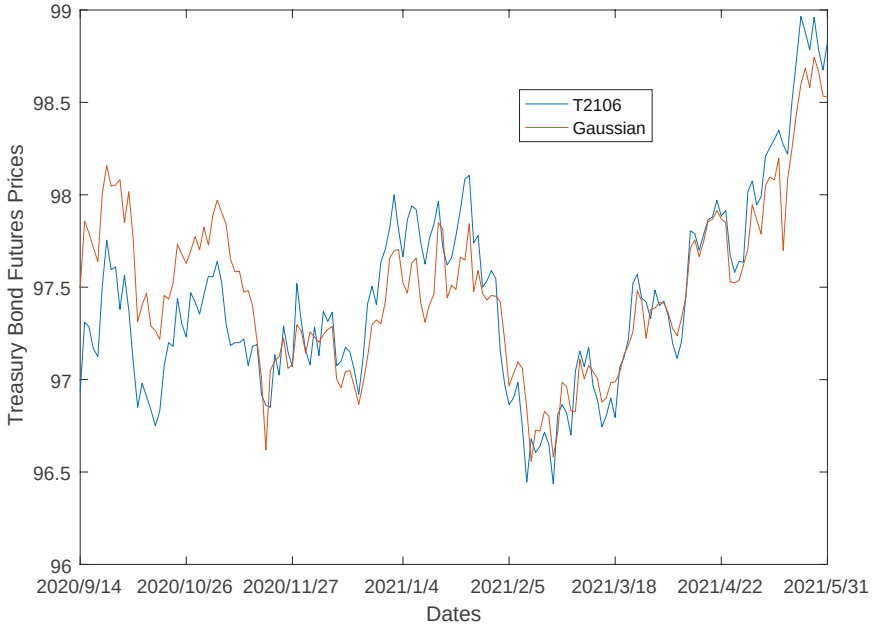

FIGURE 5 | Comparison oF Model-predicted prices and actual closing prices for T2106. [Color figure can be viewed at wileyonlinelibrary.com]

observed in other institutional contexts, policy interventions can rationally induce persistent pricing deviations by shaping market behavior and expectations (Kim 2024). In China's Treasury futures market, such interventions manifest as a systematic "policy expectation premium," particularly during strong policy-driven periods such as the clear rate-cutting cycle observed in our sample (see Figure 4). This interpretation is corroborated by tests on the T2106 contract, where the absence of a strong policy trend coincided with no systematic model bias (Figure 5).

To address this limitation, this section introduces a policy adjustment term designed to explicitly capture these institutional characteristics. The term proactively corrects the yield curve used for valuation by quantitatively incorporating the effect of policy signals, thereby enhancing model accuracy during policy-sensitive periods.

4.5.1 | *Model Modification and Adjustment Coefficient Calibration Method*

The specific modification is as follows. We replace the original yield y' used for calculating the forward valuation (Formula 7) with a policy-adjusted yield y'':

$$\begin{aligned} y'' &= y' \times (1 + R_{\text{adjust}}) \\ &= y' \times (1 + k_t(\text{MLF}_t - \text{YTM1Y}_t)), \end{aligned} \tag{21}$$

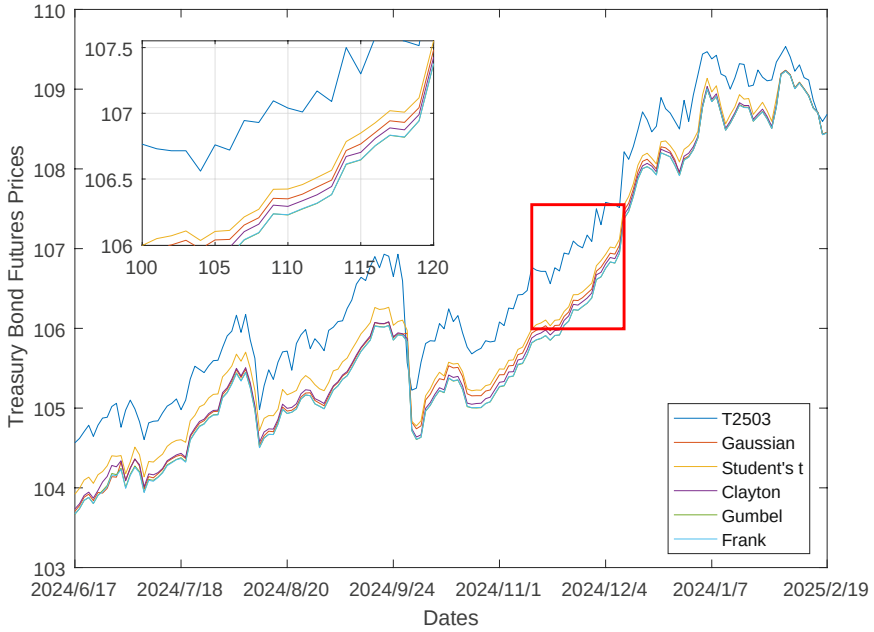

FIGURE 6 | Comparison between copula-based models in treasury futures pricing. [Color figure can be viewed at wileyonlinelibrary.com]

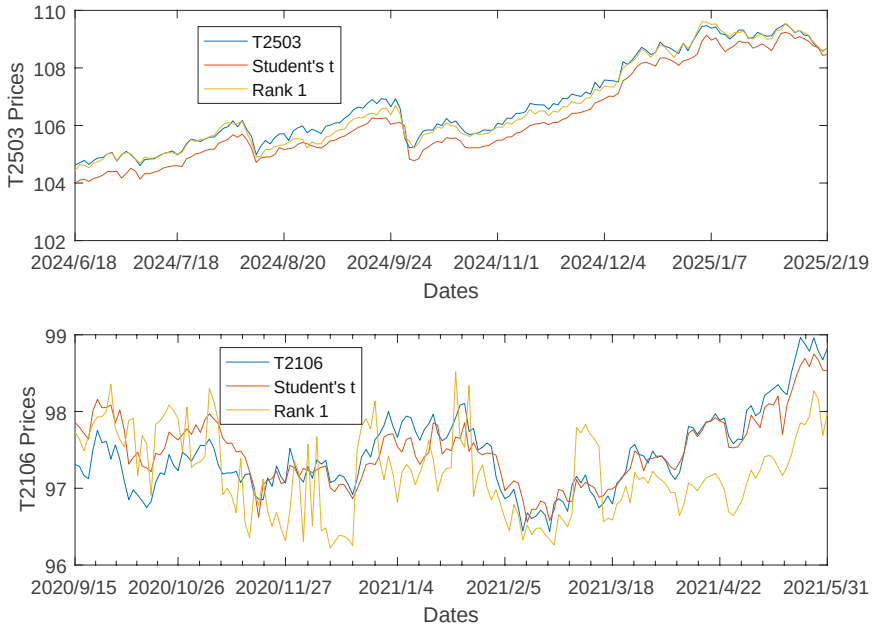

FIGURE 7 | Comparison of our model and the Nunes and Oliveira (2007) model on T2503 and T2106 contracts.[5] [Color figure can be viewed at wileyonlinelibrary.com]

where

- MLF_t is the 1-year Medium-term Lending Facility rate on pricing day t, representing the central bank's policy rate anchor.
- $YTM1Y_t$ is the 1-year Treasury bond yield to maturity on pricing day t, representing the market short-term rate.
- $MLF_t - YTM1Y_t$ spread quantifies the instantaneous deviation between the policy rate and the market rate.
- k_t is the adjustment coefficient corresponding to time t, dynamically calibrated using historical data.

The economic rationale of this adjustment term is to capture the transmission lag and intensity difference between monetary policy signals and market yields. During the rate-cutting cycle in our sample, a narrowing $MLF_t - YTM1Y_t$ spread often stems from the policy rate MLF_t decreasing more than the market yield $YTM1Y_t$. This indicates that the central bank's easing intensity is stronger than what is reflected in the current market pricing, making the bond forward valuation based on this "lagging" yield curve tend to be conservative.

Therefore, the core function of the adjustment term $k_t(MLF_t - YTM1Y_t)$ is to quantify this degree of policy surprise. By adjusting the valuation yield upward from y' to y'', it proactively

incorporates policy shocks not fully digested by the market into the model. This enables the model to output bond forward valuations more aligned with the genuine policy intent, effectively capturing the "expectation premium" induced by policy guidance.

The coefficient k_t is calibrated as follows: For pricing day t, we use the Treasury bond futures market closing price from day $t-1$ as the benchmark. An optimization algorithm solves for k_t such that the model's pricing result for day $t-1$ equals the market closing price. The calibrated k_t is then applied to the pricing for day t. For the first day of the sample period, due to lack of historical data, we set $k_1 = 0$. This dynamic calibration mechanism ensures the model can adaptively track changes in policy impact.

4.5.2 | *Empirical Test of Modification Effect*

We compared the pricing errors between the modified model (with the policy adjustment term) and the original model (Student's t-Copula) identified in Section 4.4-4, using the full sample of the T2503 contract. The results are shown in Table 10.

After introducing the policy adjustment term, all error metrics decreased significantly. The mean absolute error (MAE) decreased by 78.8%, and the minimum absolute error (Min-AE) decreased by 90.9%. This indicates that the adjustment term effectively captured and corrected the systematic undervaluation bias of the benchmark model for the T2503 contract.

The largest absolute error for the modified model occurred on September 27, 2024 (model price was 0.7504 higher than the actual closing price). On this day, the T2503 closing price dropped sharply to 105.57 from 106.60 the previous day. Because the calibration process relies on the previous day's price, the model could not promptly respond to the extreme policy shock on that day. From September 24 to 26, 2024, the People's Bank of China successively launched strong easing policies including reserve requirement ratio cuts, interest rate cuts, and reductions in existing mortgage rates. The Politburo also unusually held a meeting in September to deploy economic work, sending strong signals to stabilize growth. This shifted market sentiment rapidly from pessimistic to optimistic, causing short-term capital flows from the bond market to the stock market (In just five trading days from September 24 to 30, 2024, the Shanghai Composite Stock Index rose 21.37%), leading to abnormal volatility in bond futures prices beyond the model's normal adjustment range.

Despite this extreme case, the modified model demonstrated superior fitting performance over the entire sample. As shown in Figure 8, compared to the original model (blue solid line), the price path of the modified model (red dashed line) fits more closely to the actual market prices (green dot-dash line).

4.5.3 | *Association Between Adjustment Term and Market Interest Rate Trend*

To verify the economic significance of the adjustment term, we further analyzed the time-series characteristics of the coefficient k_t. As shown in Figure 9, k_t does not fluctuate randomly; its

TABLE 10 | Impact of policy adjustment term on T2503 contract pricing errors.

Model	MSE	MAE	Max-AE	Min-AE
Original model (Student's t-Copula)	0.2780	0.5064	0.8442	0.0167
With policy adjustment term	0.0237	0.1072	0.7504	0.0015
Improvement	91.5%	78.8%	11.1%	90.9%

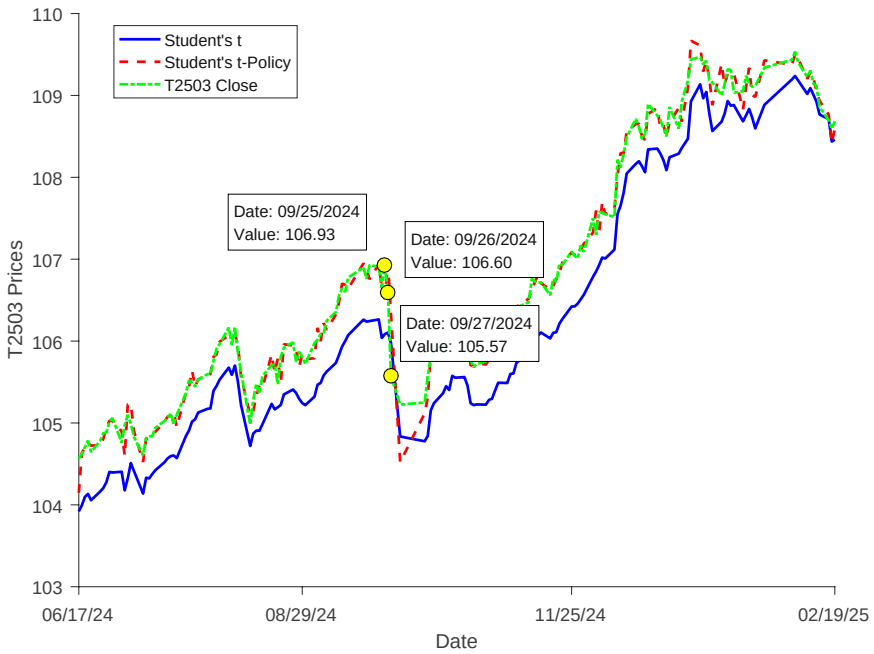

FIGURE 8 | T2503 Pricing effect comparison after introducing policy adjustment term. [Color figure can be viewed at wileyonlinelibrary.com]

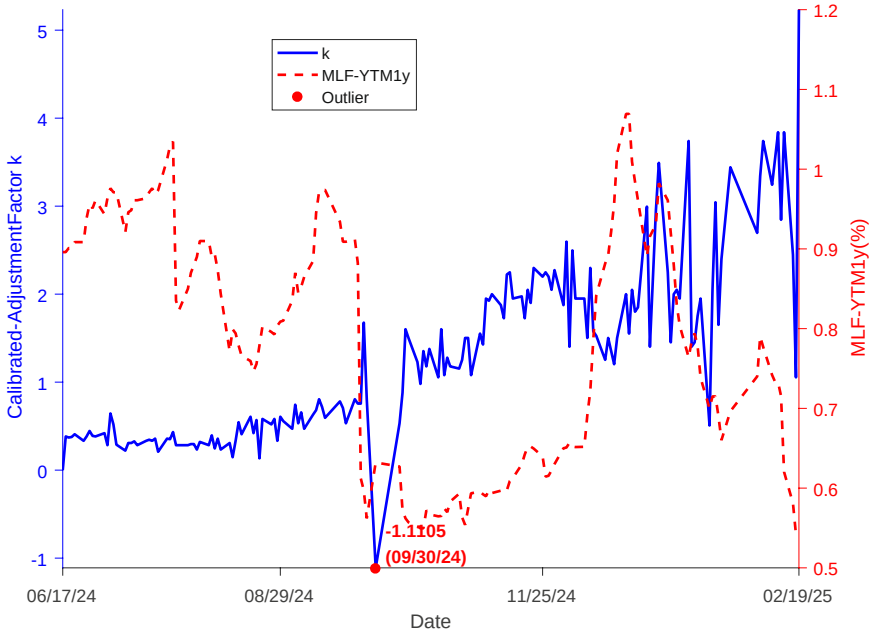

FIGURE 9 | Time-series change of adjustment coefficient k_t versus $\text{MLF}_t - \text{YTM1Y}_t$ Spread. [Color figure can be viewed at wileyonlinelibrary.com]

trend shows a clear inverse relationship with the "$\text{MLF}_t - \text{YTM1Y}_t$" sp"ead. When the spread is high, the adjustment magnitude is low; when the spread decreases, market expectations for further rate cuts strengthen, and the adjustment magnitude increases accordingly. This pattern indicates that during periods of strong policy expectations, the model requires a greater adjustment effort to align with market prices, confirming that the adjustment term successfully captures the impact mechanism of policy intervention on pricing behavior.

Additionally, an outlier appears on September 30, 2024, where the adjustment coefficient is −1.1105 (positive in other periods). This corresponds to the sharp price correction of the T2503 contract on the previous trading day (September 27, 2024), indicating that although lagged by 1 day, the market still reflected the subsequent impact of this extreme policy event through the adjustment term.

5 | Conclusion

This paper develops an innovative Treasury bond futures pricing model based on the GED-Copula framework, which successfully characterizes the heavy-tailed marginal distributions and symmetric tail dependence of valuation deviations. This core contribution offers a substantial accuracy advancement and a reliable valuation tool for market participants.

In response to the distinctive policy dynamics of the Chinese market, the model is further augmented with an adjustment term that captures policy-induced mispricing. This enhancement demonstrates the model's flexibility in incorporating institutional factors, while its primary strength remains the versatile GED-Copula foundation.

Future work will focus on integrating a broader set of market fundamentals and behavioral factors to further refine the model's performance, building upon the solid foundation established here.

Acknowledgments

We are deeply grateful to the anonymous referees for investing their valuable time and sharing their expertise to enhance the quality of this paper.

Conflicts of Interest

The author has no conflicts of interest.

Data Availability Statement

All data included in this study are provided as electronic supporting information.

Endnotes

[1] In the Treasury bond futures markets of other countries, notably the United States, an exceptional embedded option known as the "Wild Card Play" option stands out. On any deliverable day, except the final trading day, short positions are granted a window of opportunity between the official closure of Treasury bond futures trading and the deadline for submitting delivery intentions. During this period, they can use the known settlement price to search for and acquire bonds in the spot market at lower costs for delivery. China's Treasury bond futures market lacks the "Wild Card Play" option found in markets such as the United States. This is due to the synchronization of trading end times and delivery intention submission deadlines, which prevents short sellers from exploiting such opportunities.

[2] The official website of China Central Depository Clearing Co. Ltd., does not provide details about the definition of d_i. Through comparison, we selected the definition that makes the interpolation results closer to the published yields, which is $d_i = \frac{y_i - y_{i-1}}{t_i - t_{i-1}}$ and $d_{i+1} = \frac{y_{i+1} - y_i}{t_{i+1} - t_i}$.

[3] According to Musiela & Rutkowski (Corr. 3rd printing 2009, p. 432, Example 11.2.2), the parameter G should be a vector of positive

constants, while the diagonal elements of matrix a should all be negative. Note that the HJM assumption in this study differs slightly from that in the reference, resulting in differences in the sign convention. Based on these findings, we adopted the above assumptions in the subsequent parameter calibration.

[4]The paper also proposes another approximation model, the Conditional Approximation model (see Nunes & Oliveira, 2007, Theorem 1). However, the empirical results show that the performance of the Conditional Approximation model is very similar to that of the Rank 1 Approximation model. Therefore, we selected the Rank 1 Approximation model for its computational simplicity.

[5]The date range starts from the second day after the listing of the T2503 contract, as the market price of Treasury futures on the first day is used for parameter calibration, providing a basis for pricing Treasury futures on the second day. The same method is applied to the T2106 contract.

References

Abebe, T. N., and A. T. Goshu. 2024. "Asymmetric Generalized Error Distribution With Its Properties and Applications." *Frontiers in Applied Mathematics and Statistics* 10: 1398137. https://doi.org/10.3389/fams.2024.1398137.

Ampadu, S., E. T. Mensah, E. N. Aidoo, A. Boateng, and D. Maposa. 2024. "A Comparative Study of Error Distributions in the Garch Model Through a Monte Carlo Simulation Approach." *Scientific African* 23: e01988. https://doi.org/10.1016/j.sciaf.2023.e01988.

Ben-Abdallah, R., H. Ben-Ameur, and M. Breton. 2012. "Pricing the Chicago Board of Trade T-Bond Futures." *Quantitative Finance* 12, no. 11: 1663–1678.

Biagini, F., and T. Björk. 2007. "On the Timing Option in a Futures Contract." *Mathematical Finance* 17, no. 2: 267–283.

Boyle, P. P. 1989. "The Quality Option and Timing Option in Futures Contracts." *Journal of Finance* 44, no. 1: 101–113.

Broadie, M., and S. Sundaresan 1987. "The Pricing of Timing and Quality Options: An Application to Treasury Bond Futures Markets." Working Paper.

Carr, P. 1988. "Valuing Bond Futures and the Quality Option." *Working paper, University of California at Los Angeles*.

Carr, P., and R. Chen 1996. "Valuing Bond Futures and the Quality Option." Working Paper, Rutgers University.

Chang, K., and C. Zhang. 2018. "Asymmetric Dependence Structure Between Emissions Allowances and Wholesale Diesel/Gasoline Prices in Emerging China's Emissions Trading Scheme Pilots." *Energy* 164: 124–136.

Chen, R. R., and S. K. Yeh. 2012. "Analytical Bounds for Treasury Bond Futures Prices." *Review of Quantitative Finance and Accounting* 39, no. 2: 209–239.

Cohen, H. 1995. "Isolating the Wild Card Option." *Mathematical Finance* 5, no. 2: 155–165.

Coin, D. 2017. "A Goodness-of-Fit Test for Generalized Error Distribution." *Communications in Statistics-Theory and Methods* 46, no. 23: 11485–11499. https://doi.org/10.1080/03610926.2016.1271426.

Cornell, B., and K. R. French. 1983. "The Pricing of Stock Index Futures." *Journal of Futures Markets* 3: 1–14.

Fan, Y., Y. J. Zhang, H. T. Tsai, and Y. M. Wei. 2008. "Estimating 'Value at Risk' of Crude Oil Price and Its Spillover Effect Using the GED-GARCH Approach." *Energy Economics* 30, no. 6: 3156–3171. https://doi.org/10.1016/j.eneco.2008.04.002.

Fernandes, M. C., J. C. Dias, and J. P. V. Nunes. 2021. "Modeling Energy Prices Under Energy Transition: A Novel Stochastic-Copula Approach." *Economic Modelling* 105: 105671.

Gay, G. D., and S. Manaster. 1986. "Implicit Delivery Options and Optimal Delivery Strategies for Financial Futures Contracts." *Journal of Financial Economics* 16, no. 1: 41–72.

Grieves, R., and A. J. Marcus. 2005. "Delivery Options and Treasury Bond Futures Hedge Ratios." *Journal of Derivatives* 13, no. 2: 70–76.

Heath, D., R. Jarrow, and A. Morton. 1992. "Bond Pricing and the Term Structure of Interest Rates: A New Methodology for Contingent Claims Valuation." *Econometrica* 60, no. 1: 77–105.

Hemler, M. L. 1990. "The Quality Delivery Option in Treasury Bond Futures Contracts." *Journal of Finance* 45, no. 5: 1565–1586.

Jiang, T., and Q. Hua. 2019. "Option Pricing for TGARCH-M With Ged Based on Improved EEMD." *Emerging Markets Finance and Trade* 55, no. 55: 2929–2948. https://doi.org/10.1080/1540496X.2018.1561365.

Kane, A., and A. J. Marcus. 1986a. "The Quality Option in Treasury Bond Futures Market: An Empirical Assessment." *Journal of Futures Markets* 6, no. 2: 231–248.

Kane, A., and A. J. Marcus. 1986b. "Valuation and Optimal Exercise of the Wild Card Option in the Treasury Bond Futures Market." *Journal of Finance* 41, no. 1: 195–207.

Karakaş, A., A. Demİr, and S. Çalik. 2022. "Vine Copula Approach for Modelling Dependence of Commodity and Stock Markets." *Journal of Statistics and Management Systems* 25, no. 1: 1–21. https://doi.org/10.1080/09720510.2021.1877904.

Kawaller, I. G., and T. W. Koch. 1984. "Cash-and-Carry Trading and the Pricing of Treasury Bill Futures." *Journal of Futures Markets* 4, no. 2: 115–123.

Kim, J. M., D. H. Kim, and H. Jung. 2020. "Modeling Non-Normal Corporate Bond Yield Spreads by Copula." *North American Journal of Economics and Finance* 53: 101210.

Kim, R. 2024. "Hedging Securities and Silicon Valley Bank Idiosyncrasies." *Journal of Futures Markets* 44: 653–672.

Kouaissah, N., S. Ortobelli Lozza, and I. Jebabli. 2022. "Portfolio Selection Using Multivariate Semiparametric Estimators and a Copula PCA-Based Approach." *Computational Economics* 60: 833–859.

Liao, X., Z. Peng, and S. Nadarajah. 2014. "Tail Behavior and Limit Distribution of Maximum of Logarithmic General Error Distribution." *Communications in Statistics-Theory and Methods* 43, no. 24: 5276–5289. https://doi.org/10.1080/03610926.2012.730168.

Lindensjö, K. 2016. "The End of the Month Option and Other Embedded Options in Futures Contracts." *Asia-Pacific Financial Markets* 23, no. 1: 69–83.

Liu, H. H., T. K. Wang, and W. Li. 2019. "Dynamical Volatility and Correlation Among US Stock and Treasury Bond Cash and Futures Markets in Presence of Financial Crisis: A Copula Approach." *Research in International Business and Finance* 48: 381–396.

Lu, Y., X. Liao, and J. Guo. 2024. "Higher-Order Expansions of Sample Range From General Error Distribution." *Communications in Statistics-Theory and Methods* 53, no. 12: 4498–4514.

Margrabe, W. 1978. "The Value of an Option to Exchange One Asset for Another." *Journal of Finance* 33, no. 1: 177–186.

Marček, D., J. Babel, and L. Falát. 2019. "Forecasting Currency Pairs With RBF Neural Network Using Activation Function Based on Generalized Normal Distribution Experimental Results." *Journal of Multiple-Valued Logic and Soft Computing* 33, no. 6: 539–563.

Metin Karakas, A. 2019. "An Analysis of Dependence Between Oil Prices and Stock Market With Copula-GArch Approach: An Empirical Analysis From Istanbul Stock Exchange." Supplement, *Thermal Science* 23: S33–S46. https://doi.org/10.2298/TSCI180917328M.

Muganda, B. W., I. Kyriakou, and B. S. Kasamani. 2023. "Modelling Asymmetric Dependence in Stochastic Volatility and Option Pricing: A Conditional Copula Approach." *Scientific African* 21: e01765. https://doi.org/10.1016/j.sciaf.2023.e01765.

Musiela, M., and M. Rutkowski. 2009. "Martingale methods in financial modelling." In *Corr. 3rd printing 2009* (2nd ed. 2005). Springer-Verlag.

Nunes, J. P. V., and L. A. F. D. Oliveira. 2003. "Quasi-Analytical Multi-Factor Valuation of Treasury Bond Futures With an Embedded Quality Option." *Working Paper*.

Nunes, J. P. V., and L. A. F. D. Oliveira. 2007. "Multifactor and Analytical Valuation of Treasury Bond Futures With an Embedded Quality Option." *Journal of Futures Markets* 27, no. 3: 275–303.

Rendleman, R. J. 2004. "Delivery Options in the Pricing and Hedging of Treasury Bond and Note Futures." *Journal of Fixed Income* 14, no. 2: 20–31.

Ritchken, P., and L. Sankarasubramanian. 1992. "Pricing the Quality Option in Treasury Bond Futures." *Mathematical Finance* 2, no. 3: 197–214.

Yang, X. 2025. "The Embedded Option Pricing of Treasury bond Futures under GED-IO Model." *Working Paper*.

Yang, X., and L. Zhao. 2025. "Embedded Theoretical Quality Option Pricing in Treasury Bond Futures-Starting From the Definition Deviation of Conversion Factor." *International Journal of Finance & Economics* 30, no. 2: 1986–2000.

Yu, X., C. Liu, and W. Zhang. 2025. "Hedging Salmon Price Risk Based on Fuzzy Copula-Gmm Model." *International Journal of Information Technology & Decision Making* 24, no. 4: 1221–1246. https://doi.org/10.1142/S0219622023500682.

Zhang, W., X. He, and S. Hamori. 2022. "Volatility Spillover and Investment Strategies Among Sustainability-Related Financial Indexes: Evidence From the DCC-GARCH-Based Dynamic Connectedness and DCC-GARCH *T*-Copula Approach." *International Review of Financial Analysis* 83: 102223.

Zhang, Z. 2013. "Bayesian Growth Curve Models With the Generalized Error Distribution." *Journal of applied statistics* 40, no. 8: 1779–1795. https://doi.org/10.1080/02664763.2013.796348.

Zou, Y., Y. Lu, and Z. Peng. 2023. "Rates of Convergence of Powered Order Statistics From General Error Distribution." *Statistical Theory and Related Fields* 7, no. 1: 1–29.

Appendix A

Nunes and Oliveira (2007) Models and Calibration Methods

Since the empirical analysis of Nunes and Oliveira (2007) is based on a three-dimensional HJM framework, we directly adopt their Treasury futures pricing model within this framework.

1. Model Summary

1.1 HJM model:

$$\frac{dP(t,T)}{P(t,T)} = r(t)dt + \underline{\sigma}(t,T)'\bullet d\underline{W}^{\mathcal{Q}}(t), \tag{A1}$$

where $P(t,T)$ represents the time- t price of a unit face value and default-free zero-coupon bond expiring at time $T(\geq t)$; $r(t)$ is the time- t instantaneous spot rate; and $\underline{W}^{\mathcal{Q}}(t)$ is a standard Brownian motion.

Assume[3] $\underline{\sigma}(t,T)' := \underline{G}'\bullet a^{-1}\bullet[I_n - e^{a(T-t)}]$ (Nunes and Oliveira 2007, Equation 30), where $G = [G_1, G_2, G_3]$, $a = \begin{bmatrix} a_{11}, 0, & 0 \\ 0, a_{22}, 0 \\ 0, 0, a_{33} \end{bmatrix}$.

1.2 Approximate Quasi-analytical Pricing Solution (Nunes and Oliveira 2003, **working paper, Proposition 8, Equation (28)):**

$$\begin{aligned} H(t_0, T_f, \{1, ..., m\}) = \int_0^1 \Bigg\{ & \min_{j=1:m}\left[-\frac{AI_j(T_f)}{cf_j} + \sum_{i=1}^{N_j} \frac{k_i^j}{cf_j} P\left(t_0, T_f, T_i^j\right) \exp\left[-\frac{\eta\left(t_0, T_f, T_i^j\right)}{2}\right] y^{\sqrt{\varphi\left(t_0, T_f, T_i^j\right)}}\right] \\ & + \min_{j=1:m}\left[-\frac{AI_j(T_f)}{cf_j} + \sum_{i=1}^{N_j} \frac{k_i^j}{cf_j} P\left(t_0, T_f, T_i^j\right) \exp\left[-\frac{\eta\left(t_0, T_f, T_i^j\right)}{2}\right] y^{-\sqrt{\varphi\left(t_0, T_f, T_i^j\right)}}\right] \Bigg\} \\ & \frac{1}{y\sqrt{2\pi}} \exp\left[-\frac{1}{2}(\ln y)^2\right] dy. \end{aligned} \tag{A2}$$

Here, $H(t_0, T_f, \{1, ..., m\})$ represents the time-t_0 fair price of a bond futures contract with an embedded quality option, which matures at time $T_f(\geq t_0)$ and is written on a delivery basket containing m deliverable Treasury coupon-bearing bonds. $AI_j(T_f)$ denotes the accrued interest of bond j at time T_f, cf_j is the conversion factor of bond j. And N_j is the number of cash flows $k_i^j\left(i = 1, ..., N_j\right)$ paid by the jth underlying coupon-bearing bond at times $T_i^j\left(> T_f\right)$;

$$\begin{aligned} \eta\left(t_0, T_f, T_i^j\right) = \underline{G}'\bullet(a^{-1})^2\bullet\Bigg\{ & -\frac{3}{2}I_n + 2e^{a\left(T_i^j - T_f\right)} + 2e^{a(T_f - t_0)} \\ & - 2e^{a\left(T_i^j - t_0\right)} - \frac{1}{2}e^{2a\left(T_i^j - T_f\right)} + \frac{1}{2}e^{2a\left(T_i^j - t_0\right)} \\ & - \frac{1}{2}e^{2a(T_f - t_0)}\Bigg\}\bullet a^{-1}\bullet\underline{G}; \end{aligned}$$

$$\begin{aligned} \varphi\left(t_0, T_f, T_i^j\right) = \underline{G}'\bullet 1/2\bullet(a^{-1})^2\bullet[e^{2a(T_f - t_0)} - I_n]\bullet\left[e^{a\left(T_i^j - T_f\right)} - I_n\right]^2 \\ \bullet(a^{-1})'\bullet\underline{G}; \end{aligned}$$

1.3 Proposition assumption (Rank 1 approximation, upper bound) model[4] (Corollary 1 in Nunes and Oliveira (2007)**)**

$$\begin{aligned} H^u(t_0, T_f, \{1, ..., m\}) &= E_Q\left\{\min_{j=1:m} E_Q\left(\frac{CB_j(T_f)}{cf_j}|Z\right)|\mathcal{F}_{t_0}\right\} \\ &= \sum_{j=1}^{m} \frac{AI_j(T_f)}{cf_j} I_{jk}\left[\Phi\left(z_{k-1}^*\right) - \Phi\left(z_k^*\right)\right] \\ &\quad + \sum_{j=1}^{m}\sum_{i=1}^{N_j} \frac{k_i^j}{cf_j} F\left(t_0, T_f, T_i^j\right)\omega_{ji}. \end{aligned} \tag{A3}$$

Here, $F\left(t_0, T_f, T_i^j\right) = P\left(t_0, T_f, T_i^j\right)\exp\left[-\frac{\eta\left(t_0, T_f, T_i^j\right)}{2} + \frac{1}{2}\varphi\left(t_0, T_f, T_i^j\right)\right]$;

$P\left(t_0, T_f, T_i^j\right) := \frac{P\left(t_0, T_i^j\right)}{P(t_0, T_f)}$ defines the time-t_0 forward price for delivery at time T_f of a risk-free pure discount bond with maturity at time T_i^j; and $\Phi(\bullet)$ is the CDF of the standard normal distribution.

$-\infty = z_0^* < z_1^* < z_2^* < ... < z_r^* < z_{r+1}^* = +\infty$ are all possible solutions in z for the set of nonlinear equations: $\frac{CB_j(T_f;z)}{cf_j} = \frac{CB_l(T_f;z)}{cf_l}, j = 1:m-1, l = j+1:m$. Where

$$\frac{CB_j(T_f;z)}{cf_j} := -\frac{AI_j(T_f)}{cf_j} + \sum_{i=1}^{N_j} \frac{k_i^j}{cf_j} P\left(t_0, T_f, T_i^j\right) \exp\left[-\frac{\eta\left(t_0, T_f, T_i^j\right)}{2} + \sqrt{\varphi\left(t_0, T_f, T_i^j\right)} z\right];$$

$$I_{jk} := 1_{\left\{\frac{CB_j(T_f;z)}{cf_j} \le \frac{CB_l(T_f;z)}{cf_l}, \forall l \ne j, \forall z \in \left[z_{k-1}^*, z_k^*\right]\right\}};$$

$$\omega_{ji} := \sum_{k=1}^{r+1} I_{jk} \left\{\Phi\left[z_k^* - \sqrt{\varphi\left(t_0, T_f, T_i^j\right)}\right] - \Phi\left[z_{k-1}^* - \sqrt{\varphi\left(t_0, T_f, T_i^j\right)}\right]\right\};$$

2. Parameters Calibration methods

In the empirical analysis, Nunes and Oliveira (2007) adopted a two-stage calibration approach:

Stage 1: On each sample day, the term structure of interest rates is estimated by minimizing the mean absolute percentage error (MAPE) between the fitted bond prices and the market prices of coupon-bearing bonds. In this stage, nine parameters from Nunes and Oliveira (2007, Equation 31) are calibrated, namely z_1, z_2, z_3, z_4, z_5, z_6, a_{11}, a_{22} and a_{33}.

Stage 2: The parameters G_1, G_2, and G_3 are calibrated by comparing the market prices of Treasury futures with the model prices.

In our approach, we directly utilize the market prices of Treasury futures to calibrate G_1, G_2, G_3, a_{11}, a_{22} and a_{33} by Model (A.2), and then employ Model (A.3) to price Treasury futures. Specifically, when pricing Treasury futures on a given day, we first use the market prices of Treasury futures from the previous day to calibrate the parameters through Model (A.2). The calibrated parameters are then substituted into the approximate Model (A.3) to compute the pricing results for the current day.